TAMPEREEN TEKNILLINEN YLIOPISTO
TAMPERE UNIVERSITY OF TECHNOLOGY

JAAKKO MÄHÖNEN

VALIDATION OF TEST METHODS FOR FILTERS ON GAS ENGINE APPLICATIONS

Master of Science Thesis

Examiner: Professor Kalevi Huhtala
Examiner and subject approved on 8st of August 2018

ABSTRACT

JAAKKO MÄHÖNEN: Validation of test methods for filters on gas engine applications
Tampere University of Technology
Master of Science Thesis, 51 pages, 1 Appendix page
August 2018
Master's Degree Programme in Automation Technology
Major: Hydraulics and Automation, Fluid Power
Examiner: Professor Kalevi Huhtala

Keywords: filtration, testing, gas filter, air filter, testing method, validation, natural gas, standard, simulation model, filtration efficiency, pressure loss

To be able to choose the right filter for specific application, filters need to be validated. Validation of filters will give essential information about the filter's capability, e.g. filtration efficiency, pressure loss and dirt holding capacity. Validation is done according to a standard, which describes in detail level the testing method and the test rig. There are many different standards for air filters, however, no standards designed for filters on natural gas applications. Therefore, air filter standards and the test rigs described in them must be used to validate filters on natural gas applications.

To understand the effects of different gas types and their properties better, understanding the theory of gas filtration is essential. According to many studies, there are several different filtration mechanisms in gas filtration. Each of these mechanisms can be simulated with mathematical calculations. Combining these calculations into a single simulation model will offer a theoretical way to investigate filters' capability. The simulation model will simulate the filtration efficiency and the pressure loss of the selected filter media. The model can be also used to compare the filtration results when using different types of gases.

Also the simulation model needs to be validated to get knowledge about the accuracy of the model. The validation of the model was done by comparing the simulation results with actual test results received from a test rig in Parker Hannifin's laboratory. The validation reveals that the simulation model works more accurately with some of the filter medias. With coarse filter medias the simulation results are reasonably accurate, but with finer medias the simulation results will suffer slightly.

The simulation model can be used to test different kinds of filter medias. Filter medias can be simulated in different environmental conditions (temperature, pressure), with different flow velocity and with different kind of dirt particles. The simulation model also offers information about the effectiveness of the different filtration mechanisms, and it can be used as a guide when designing new filters and when developing filter medias.

TIIVISTELMÄ

JAAKKO MÄHÖNEN: Validation of test methods for filters on gas engine applications
Tampereen teknillinen yliopisto
Diplomityö, 51 sivua, 1 liitesivu
Elokuu 2018
Automaatiotekniikan diplomi-insinöörin tutkinto-ohjelma
Pääaine: Hydrauliikka ja automatiikka, hydraulitekniikka
Tarkastaja: professori Kalevi Huhtala

Avainsanat: suodatus, testaus, kaasusuodatin, testimenetelmä, maakaasu, standardi, simulointimalli, suodatustehokkuus, painehäviö

Suodattimien validointi mahdollistaa oikeanlaisen suodattimen valinnan käyttökohteen mukaan. Validointi antaa tietoa suodattimen kyvykkyydestä, muun muassa suodatustehokkuudesta, painehäviöstä ja likakapasiteetista. Validointi toteutetaan standardien avulla, jotka sisältävät yksityiskohtaista tietoa testimenetelmistä sekä testaukseen käytettävästä testipenkistä. Ilmasuodattimille on olemassa useita eri standardeja, mutta maakaasukäytössä oleville suodattimille ei erillisiä standardeja löydy, joten niiden validointiin on käytettävä ilmakäyttöön suunniteltuja standardeja.

Kaasusuodatuksen teorian avulla saadaan tietoa eri kaasujen ja niiden ominaisuuksien vaikutuksesta suodattimen toimintaan. Tutkimusten mukaan kaasusuodatuksen katsotaan koostuvan useista eri suodatusmekanismeista. Suodatusmekanismeja voidaan simuloida matemaattisten kaavojen avulla, ja yhdistämällä nämä eri mekanismeja kuvaavat kaavat yhdeksi kokonaisuudeksi, voidaan suodattimien kyvykkyyttä tutkia teorian kautta matemaattisen simulointimallin avulla. Simulointimallilla voidaan mallintaa valitun suodatusmateriaalin suodatustehokkuus sekä painehäviö. Simulointimallilla voidaan myös vertailla eri kaasujen vaikutusta suodatustuloksiin.

Jotta saataisiin käsitys simulointimallin tarkkuudesta, tulee se validoida. Malli validoitiin vertailemalle siitä saatuja tuloksia Parker Hannifinin laboratorion testipenkistä saatuihin tuloksiin. Validoinnin perusteella simulointimalli toimii joillakin suodatusmateriaaleilla paremmin kuin toisilla. Harvemmilla suodatusmateriaaleilla simulointitulokset vastaavat hyvin testipenkistä saatuja tuloksia, mutta tiheämmillä suodatusmateriaaleilla tulosten välillä syntyi enemmän eroa.

Simulointimallia voidaan käyttää eri suodatusmateriaalien testaukseen. Suodatusmateriaaleja voidaan simuloida eri ympäristöolosuhteissa (lämpötila, paine), eri virtausnopeuksilla sekä erityyppisillä likapartikkeleilla. Simulointimalli antaa myös tietoa eri suodatusmekanismien keskinäisestä suhteesta, ja sitä voidaan käyttää apuna uusien suodatinten suunnittelussa sekä suodatinmateriaalien kehitystyössä.

PREFACE

This Master of Science Thesis is done for Parker Hannifin Manufacturing Finland Oy. The completion of this work has required contacting lots of different people, and I want to thank all of them for their help. Especially I want to thank Mr. Petteri Kapanen and Mr. Antti Sorri from Parker Hannifin for their support for my thesis, and also the whole laboratory and R&D teams of Urjala. Special thanks belongs to Dr. Jürgen Timmler who introduced me to many important contacts in Filtec exhibitions in 2016, and to Dr. Wolfgang Mölter-Siemens and Dr. Stefan Haep from IUTA who offered me the template of the filtration simulation model.

Besides these, I want to thank professor Kalevi Huhtala for examining my study. Warm thanks also to my wife Minna for motivating me on my work, and to my son Tuomo for keeping my mind fresh by giving me other things to think about besides my thesis.

Tampere, June 20th 2018

Jaakko Mähönen

CONTENTS

TABLE OF FIGURES

TERMS AND DEFINITIONS

Δp	Pressure loss [Pa]
A_m	Average arrestance
C_c	Slip correction factor
CGS	City gate station
CNC	Condensation nucleus counter
CNG	Compressed natural gas
D	Diffusion coefficient
DEHS	Di-Ethyl-Hexyl-Sebacat
d_f	Fiber diameter [m]
d_p	Particle diameter [m]
E	Filtration efficiency of the filter
E_D	Efficiency due to diffusion
$E_{D,sf}$	Single fiber efficiency due to diffusion
E_{DR}	Efficiency due to interception and diffusion combined
$E_{DR,sf}$	Single fiber efficiency due to interception and diffusion combined
E_G	Efficiency due to gravitation
$E_{G,sf}$	Single fiber efficiency due to gravitation
E_I	Efficiency due to inertial impaction
$E_{I,sf}$	Single fiber efficiency due to inertial impaction
E_m	Average efficiency
EN 1822	EN 1822:2009 – High efficiency air filters (EPA, HEPA and ULPA)
EN 779	EN 779:2012 - Particulate air filters for general ventilation – Determination of the filtration performance
EPA	Efficient particulate air filter
ePM_x	Class specified by ISO 16890:2016
E_R	Efficiency due to interception
$E_{R,sf}$	Single fiber efficiency due to interception
Eurovent 4/9	Eurovent 4/9:1997 - Method of testing air filters used in general ventilation for determination of fractional efficiency
$E_{\Sigma,sf}$	Total single fiber efficiency
$E_{\Sigma e,sf}$	Total single fiber efficiency due to electrical force
$E_{\Sigma m,sf}$	Total single fiber efficiency due to mechanical force
$E_{\Sigma m,e}$	Total single fiber efficiency including mechanical and electrical force
F_d	Drag force
F_E	Total electrostatic force
F_{EC}	Coulombic force between charged particles and charged collectors
F_{EI}	Electric image force between charged particles and neutral collectors
F_{EM}	Electric image force between neutral particles and charged collectors
F_{ES}	Particle charged in the same sign produces a repulsive force among themselves
F_{EX}	Force on charged particles in the presence of a neutral collector by a uniform external electric field
F_{icp}	Electric dipole interaction force between an uncharged particle and an uncharged collector both being polarized by an external electric field
G	Gravitation parameter
g	Gravitational constant

GTL	Gas to liquid
GTS	Gas to solid
GTW	Gas to wire
HEPA	High efficiency particulate air filter
HVDC	High-voltage direct current
IPA	Isopropanol
ISO 16890	ISO 16890:2016 – Air filters for general ventilation
IUTA	Institute of Energy and Environmental Technology
J	Experimental parameter
k	Boltzmann constant [J/K]
Kn_p	Knudsen number
K_u	Kuwabara hydrodynamic factor
KCI	Potassium chloride
LNG	Liquefied natural gas
M	Molar mass [kg/mol]
MPPS	Most penetrating particle size
N_R	Ratio of particle and fiber diameter
OPC	Optical particle counter
P	Fraction of unfiltered dirt particles
p	Pressure [Pa]
PAO	Poly alpha olefin
P_D	Portion of the particles not filtered due to diffusion
P_{DR}	Portion of the particles not filtered due to interception and diffusion combined
Pe	Peclet number
P_G	Portion of the particles not filtered due to gravitation
P_I	Portion of the particles not filtered due to inertial impaction
P_R	Portion of the particles not filtered due to interception
PSL	Polystyrene latex
Q	Flow [m^3/s]
Q_f	Quality factor
R	Gas constant [$\frac{j}{mol*K}$]
Stk	Stokes number
T	Temperature [K]
t	Thickness of the filter [m]
TBS	Town border station
U_0	Filtration face velocity [m/s]
ULPA	Ultra-low penetration air filter
α	Packing density of the filter
γ	Adhesion probability
η	Filter efficiency
η_C	Capturing efficiency
λ	Mean free path [m]
μ	Dynamic viscosity [kg/ms]
ρ_g	Gas density [kg/m^3]
ρ_p	Particle density [kg/m^3]

1. ABOUT THIS STUDY

Even though the popularity of the renewable energy sources is growing, there are still demands for fossil fuels. Among fossil fuels, natural gas is the most energy efficient, and it offers energy savings compared to oil or coal. Natural gas is used in a wide range of different kinds of applications. It is used for e.g. electricity generation, as a transportation fuel, a source for chemicals, and also in private homes for cooking and heating. Natural gas has strengthened its position in the world's energy markets, and its role is expected to grow significantly in the future. (Mokhatab, et al., 2015, pp. 1-2) The fundamentals of natural gas are presented in chapter 2 including composition of natural gas, processing the gas and transportation methods.

Natural gas contains lots of different sorts of impurities when leaving from the wells. These impurities include e.g. unwanted gas compounds, moisture, and solid dirt particles. Because of the impurities, natural gas must be processed and treated before its commercial use. (Mokhatab, et al., 2015, p. 33) Filtrating solid dirt particles from the gas with gas filters is an essential part of the gas treatment process.

To be able to choose the right filter for the right place, filters need be validated, and for this purpose there are different standards. The standards contain detailed specifications of test rigs, which are used to validate the filters. There are no specific standards for filters in natural gas applications, and therefore standards designed for air applications must be used. These standards are introduced in chapter 3.

The theory of gas filtration has been studied in numerous different publications. These publications have introduced several different filtration mechanisms, and each of these mechanisms have their own individual functionality and characteristics. The different filtration mechanisms are presented in chapter 4.

Based on the gas filtration theory and the different filtration mechanisms, a mathematical simulation model is introduced in chapter 5. The simulation model is built based on mathematical formulas from several studies. The model simulates filtration efficiency and the pressure loss of the chosen filter media. There are several different input parameters which can be varied, e.g. temperature, pressure and the type of gas. Because there are not any test rigs commercially available for filters in natural gas applications, this simulation model can be used as a guide to have a better understanding about the effects of the gas properties to filter performance.

In chapter 6 the simulation model is validated using actual test results from a test rig located in a laboratory in Parker Hannifin's Urjala location. The test results from the laboratory are compared with the results from the simulation model, and the comparison of the results will give information about the accuracy of the model. The differences between the simulation and test rig results are also analyzed. In chapter 7 the study is summarized, and conclusions are presented.

2. NATURAL GAS

Natural gas is a gaseous fossil fuel, which origins from remains of animals and plants. Over time, pressure and heat has transformed the remains into natural gas, which is nowadays used as an energy source. (Speight, 2007, p. 3) Natural gas consists mainly of methane, and it is the most energy efficient fossil fuel (Mokhatab, et al., 2015, pp. 1-3). Natural gas occurs as accumulations in different kinds of geological traps, and it is collected from the accumulations with various technologies. (Guo & Ghalambor, 2005, p. 1)

2.1 Natural gas composition

Natural gas is mainly used as a fuel, and its use as an energy source is based on its heating value gained by burning the gas. The heating value of natural gas depends on the types and amount of the gases it contains. (Mokhatab, et al., 2015, p. 6) Natural gas consists mainly of methane. Other gases natural gas usually consists are ethane, propane, butane, nitrogen and carbon dioxide. The composition of natural gas varies largely depending on the source of the gas, and in Table 1 is shown different compositions of natural gas collected from different locations. (Suomen Kaasuyhdistys ry, 2014, p. 6)

Table 1. *Composition of natural gas from different sources (Suomen Kaasuyhdistys ry, 2014, p. 6)*

	Russian Urengoi	**Germany Goldenstedt**	**USA Kansas**	**Netherlands Groningen**	**Norway Troll**
Methane CH_4	98 %	88,0 %	84,1 %	81,3 %	93,2 %
Ethane C_4H_6	0,8 %	1,0 %	6,7 %	2,8 %	3,7 %
Propane C_3H_8	0,2 %	0,2 %	0,3 %	0,4 %	0,4 %
Butane C_4H_{10}	0,02 %	-	-	0,4 %	0,5 %
Nitrogen N_2	0,9 %	10,0 %	8,4 %	14,3 %	1,6 %
Carbon dioxide CO_2	0,1 %	0,8 %	0,8 %	0,9 %	0,6 %

2.2 Natural gas processing

The natural gas acquired from the gas wells, i.e. raw gas, must be processed and treated before it can be transferred via pipe lines. In case the contamination level of the gas is low and there are little acid gases, the gas can be sent directly to the sales pipeline after treatment and drying at the wellhead. With more contaminated gas, the gas must be collected to a separate gas-processing plant where it is treated, conditioned and dried. (Mokhatab, et al., 2015, p. 33)

The target of the purification process is to obtain high-methane gas with no unwanted contaminants such as acid gases, heavy hydrocarbons, nitrogen, water or other impurities. Furthermore, the processed gas must meet the requirements set for heating values, to be able to ensure the optimal operation of gas turbines and to minimize emissions of combustion equipment. Some of the removed impurities of the natural gas can be collected and used for other purposes. For example, propane and butane can be used as liquefied petroleum gas, and ethane as a feedstock to petrochemical plants. (Mokhatab, et al., 2015, pp. 123-124)

Even after the gas is pure enough to be able transfer via pipelines, it still needs to be purified further before end users can use it. The cleanliness of the natural gas depends heavily on which part of the gas's transportation network the samples are taken. The closer to the end user the sample is taken, the cleaner it usually is. This can be clearly seen in the following example of a gas distribution in an urban city in Figure 1. (Azadi, et al., 2011, pp. 1166-1167)

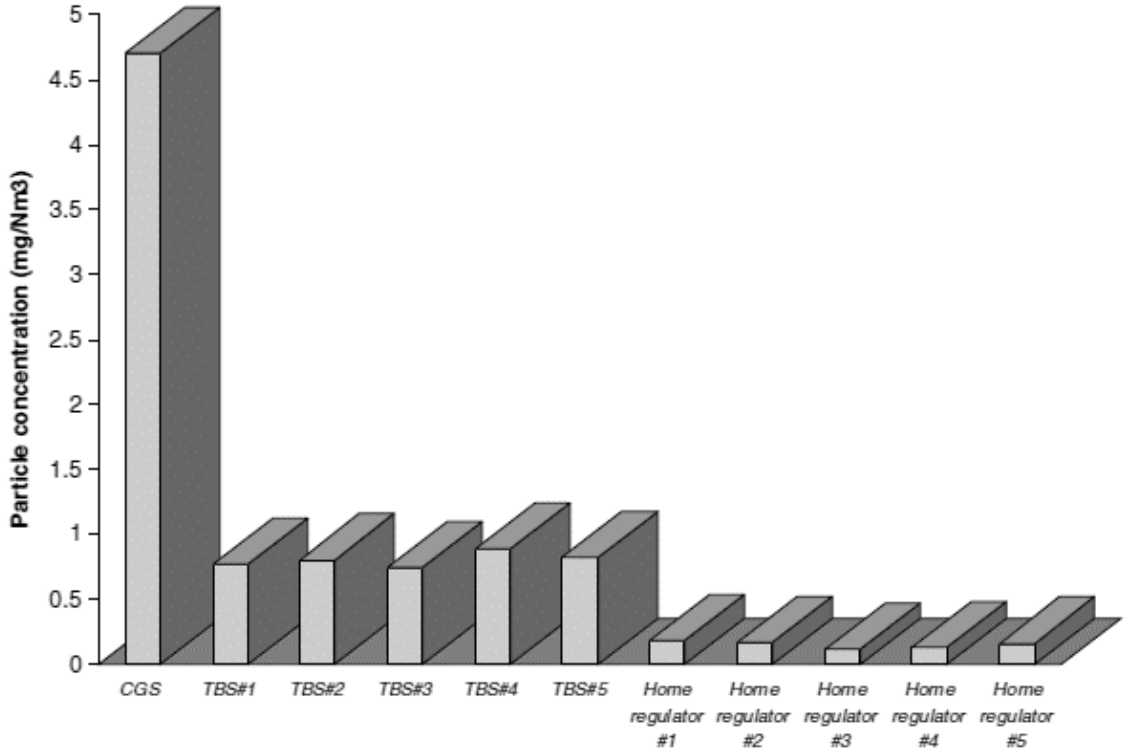

Figure 1. *Dirt particle concentration of an urban city at various sampling points (Azadi, et al., 2011, p. 1168)*

In Figure 1 is shown the cleanliness of natural gas in three different stages at an urban city's natural gas distribution. City gate station (CGS) is the main natural gas pipeline of the city, and the gas has lots of impurities at this stage. Town border stations (TBS) are medium sized distribution stations which distribute the gas to individual homes (Home regulators). The gas's dirt particle concentration is significantly lower in town border stations compared to city gate station, and cleanliness is increased further when measured from home regulators. Gas is filtered along the transportation network, and when coming closer to the end user, the filters will be finer.

2.3 Natural gas transportation

Natural gas reserves occur regularly far from the markets where it is used. It must be gathered, processed and transported before getting it to these markets. Traditionally the gas from the wells have been transported to the markets via pipeline network. Other common method is to transport the gas as liquefied natural gas (LNG). Nowadays, there are

also other solutions for the transportation, however some of these solutions still require further efficiency improvements and others further technology development before being commercially reasonable alternatives. (Mokhatab, et al., 2015, pp. 24, 37) The different transportation methods are visualized in Figure 2:

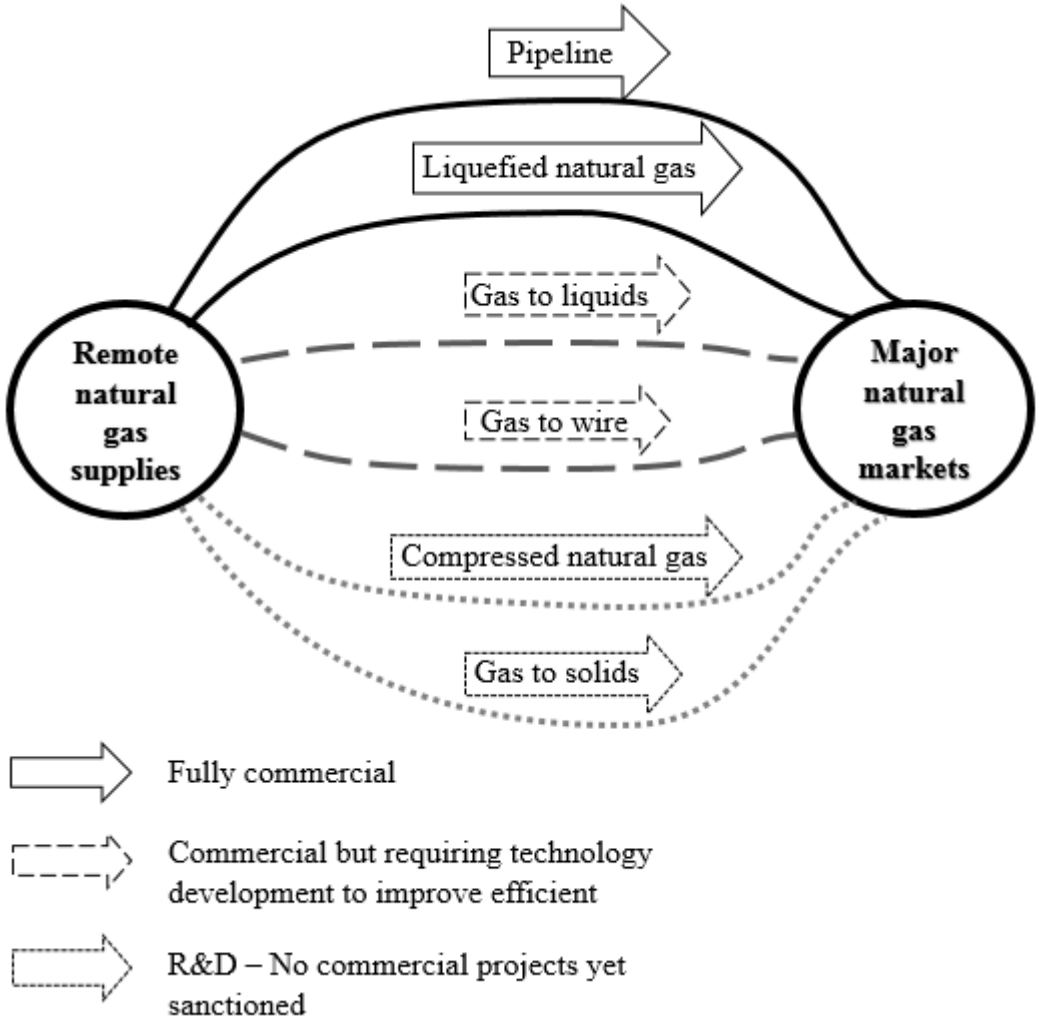

Figure 2. *Technologies available to transport natural gas over long distances (Wood, et al., 2008, p. 2)*

2.3.1 Transportation methods in commercial use

Natural gas transportation via pipeline network is a convenient and stable method. However, because the pipelines are usually thousands of kilometers long and they often pass through many different countries, there might be some political or economic uncertainties. In addition, the majority of the large and easy-to-produce gas wells have already been used, and therefore it has been obligatory to build gas wells also to more challenging environments with fewer gas reserves. Because of the high initial investments, that is needed for the construction of the pipelines, it may not be commercially profitable to transport the gas via pipelines from the smaller wells. (Mokhatab, et al., 2015, pp. 24-25)

The other widely used transportation method for natural gas is transporting it as liquefied natural gas (LNG). When natural gas is cooled to -162 °C temperature, the volume of it is reduced to approximately $1/600^{th}$ of the original volume. Because of the significantly lower volume, gas can be transported with tanker ships and trucks, which is more cost efficient method than pipelines. However, the costs of liquefying the gas can be high. (Mokhatab, et al., 2015, p. 26)

2.3.2 Transportation methods under pilot use

Transporting natural gas converted to liquid is called gas-to liquids (GTL). In this method the methane is mixed with steam and is converted to syngas using a catalyst technology. Syngas is then transformed to liquid using Fischer-Tropsch process or an oxygenation method. Although there are already many environmental benefits with GTL, the energy efficiency of the syngas generation is still low. Therefore, further investigations are needed to improve the energy efficiency and to lower the cost of this method. (Mokhatab, et al., 2015, p. 27)

Natural gas is widely used as a fuel for electricity generation. If the natural gas would be used to produce electricity in a power plant nearby the gas well, it could be transported to end markets formed as electricity instead of gas. This kind of transportation method is called gas-to-wire (GTW). Transporting electricity via HVDC transmission lines has low losses, <10 %, and hence it is the most technically viable solution to move electricity over long distances. However, building a power plant to a remote site near the gas well requires big capital investments and also the maintenance costs are high. For these reasons GTW still need further development. (Mokhatab, et al., 2015, pp. 29-30)

2.3.3 Transportation methods not yet in commercial use

One potential future method of natural gas transportation is to transport it in high pressure containers. The gas is pressurized in these containers up to ~125 – 250 bars, and therefore the volume of the gas is significantly smaller. Because lack of liquefying process, it can be more economical solution than LNG. Transporting the gas as compressed natural gas (CNG) will need appropriate ships which are designed for this use. (Mokhatab, et al., 2015, pp. 26-27)

Transporting natural gas in a form of gas hydrates is called gas-to-solid (GTS). In this method natural gas is combined with water and then set under high pressure and low temperature. Under these conditions natural gas is “frozened” to solid state. The benefit of GTS is that it requires only -20 °C temperature compared to LNG’s -162 °C, and requires therefore less investments to produce and transport. However, one cubic meter of GTS contains only 160 Nm^3 of natural gas compared to LNG’s 600 Nm^3, and for that reason it requires a lot more space in transport, leading to higher costs. (Mokhatab, et al., 2015, pp. 28-29)

3. STANDARDS

The performance of filters can be tested according to standards. However, there are no separate standards for validating industrial filters which are used to remove particulate matters from gases other than air. Therefore, these kinds of filters must be validated using standards designed for air applications. Because of this, the test results will not be 100 % accurate. However, the differences in filtration efficiency, for example between air and natural gas as a fluid, are relatively small.

Standards EN 779 and EN 1822 have been commonly used in Europe for air filtration validation. However, a new international standard ISO 16890 has superseded the EN 779 after the transition time ended in June 2018, and EN 779 is no longer officially active (Courtey, 2017, p. 17). Eurovent 4/9:1997 -standard is not widely used, but Parker Hannifin's test rig in Urjala laboratory is based on it.

Even though all these standards are used for air filter validation, there are many differences between the standards. For instance, the testing rig used in the tests depends on the used standard. Also the test methods described on the standards give slightly different type of results depending on the used standard, and these might not be comparable to the results received from a different standard. Regardless of these differences, all the standards give a good view of the performance level of the tested filter. With a rating system which each of these standards provide, it is easy to compare different filters, as long as all the filters are tested according to the same standard.

3.1 EN 779:2012 – Particulate air filters for general ventilation – Determination of the filtration performance

EN779:2012 applies to filters having an efficiency of <98 % with particles sized 0,4 µm. This standard is used to determine the average filtration efficiency and the average weight arrestance of the filter. (Wilcox, et al., 2010, pp. 81-82)

3.1.1 Testing process and test rig

The basic idea of the filtration efficiency test is simple. The test aerosol (DEHS) is dispersed evenly across the duct upstream of the filter. There are sampling heads in both sides of the testing rig; before and after the filter. These sampling heads gather samples that are analyzed by an optical particle counter (OPC). With the gathered data the efficiency of the tested filter can be evaluated. The testing rig is shown on Figure 3.

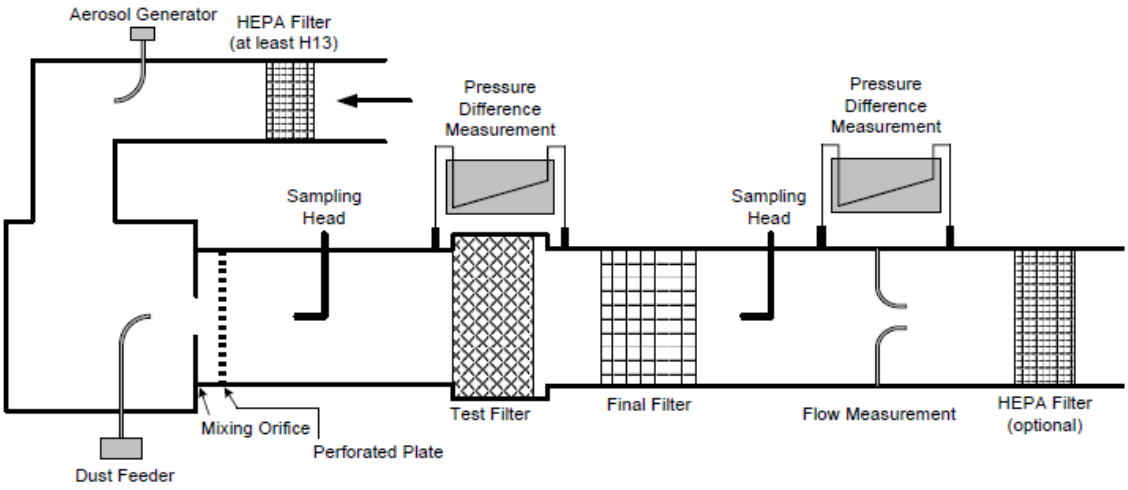

Figure 3. *Schematic of EN 779:2012 (Wilcox, et al., 2010, p. 83)*

There are two different substances used in the testing of the filters. One is used to evaluate the efficiency of the filter and other one is used to evaluate the dust holding capacity. For filter efficiency test, Di-Ethyl-Hexyl-Sebacate (DEHS) is used. It is a neutral liquid test aerosol and optical particle counter works more accurate with it compared to solid test particles. (Wilcox, et al., 2010, p. 83)

To evaluate the dirt holding capacity of the filter, there are two different test dusts mentioned in the standard. ASHRAE test dust is used for "coarse" filters and ISO 12103 is used for "fine" filters. (Wilcox, et al., 2010, p. 83)

Before inserting any of the test particles to the testing rig, the initial pressure loss of the filter should be measured. After it is measured, it should be determined if the filter efficiency will be dependent on the electrostatic charge of the filter. After these tests the filter efficiency test and the dust holding capacity test can be performed. (Wilcox, et al., 2010, p. 84)

3.1.2 Classification system

In the classification system of EN779:2012 there are three groups: F, M and G. (EN 779:2012, p. 5) The classification of the filters will be done under following test conditions: Air flow Q = 0,944 m^3/s (3400 m^3/h), maximum final test pressure drop Δp = 250 Pa with coarse filters (group G) and Δp = 450 Pa with medium or fine filters (groups M and F). (EN 779:2012, p. 14)

Filters are rated to group G if they have the average efficiency less than 40 % with 0,4 µm particles. The sub-classification to groups G1-G4 is based on the filter's dust holding capacity. (EN 779:2012, p. 5)

Group M consists filters that have an average efficiency value between 40 % - 80 % with 0,4 µm particles. Unlike in the group G, the sub-classification of M-filters (M5 or M6) is

based on the filter's average efficiency with 0,4 µm particles instead of the filter's dust holding capacity. (EN 779:2012, p. 5)

Filters with an average efficiency >80 % of 0,4 µm particles are included in group F. The sub-class (F7-F9) depends on their average efficiency with 0,4 µm particles, but also to the minimum efficiency during the test. (EN 779:2012, p. 5)

Different classes and their requirements are shown on Table 2.

Table 2. *Classification of air filters according to EN 779:2012 (EN 779:2012, p. 14)*

Group	**Class**	**Final test pressure drop [Pa]**	**Average arrestance (A_m) of synthetic dust [%]**	**Average efficiency (E_m) of 0,4 µm particles [%]**	**Minimum efficiency of 0,4 µm particles [%]**
Coarse	G1	250	$50 \leq A_m < 65$	-	-
	G2	250	$65 \leq A_m < 80$	-	-
	G3	250	$80 \leq A_m < 90$	-	-
	G4	250	$90 \leq A_m$	-	-
Medium	M5	450	-	$40 \leq E_m < 60$	-
	M6	450	-	$60 \leq E_m < 80$	-
Fine	F7	450	-	$80 \leq E_m < 90$	35
	F8	450	-	$90 \leq E_m < 95$	55
	F9	450	-	$95 \leq E_m$	70

3.2 ISO 16890:2016 – Air filters for general ventilation

ISO 16890 standard replaced standard EN 779 completely after transition period ended in June 2018. There are many differences between these two standards, and the new ISO 16890 have many benefits compared to EN 779. ISO 16890 will be widely used across the world, and the new approach for classification system and testing gives more reliable results, which are closer to the results in the filter's actual use. (ISO 16890:2016, Part 1, 2016, p. 5)

ISO 16890 standard consists of four different parts:

- Part 1 – Technical specifications, requirements and classification system based upon particulate matter efficiency (ePM)
- Part 2 – Measurement of fractional efficiency and air flow resistance
- Part 3 – Determination of the gravimetric efficiency and the air flow resistance versus the mass of test dust captured
- Part 4 – Conditioning method to determine the minimum fractional test efficiency

3.2.1 Testing process and test rig

The filtration efficiency is measured by using particles sized 0,3 µm to 10 µm, with a test rig illustrated in Figure 4. (ISO 16890:2016, Part 2, 2016, p. 5)

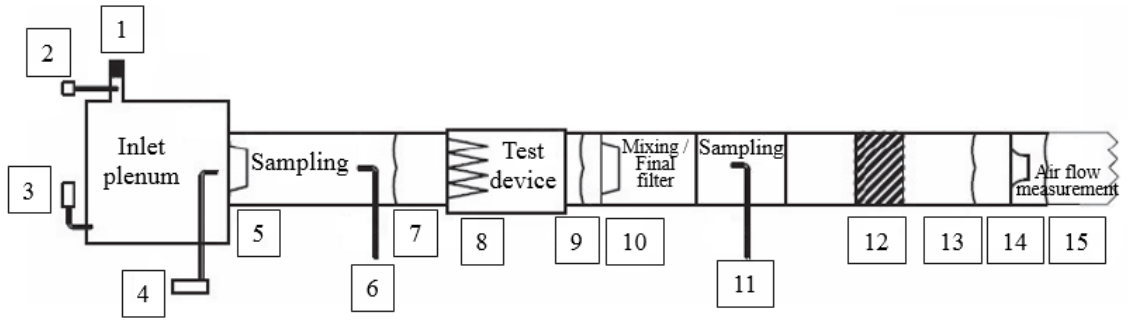

1. HEPA filtration
2. Liquid aerosol injection
3. Solid aerosol injection
4. Dust injection nozzle
5. Mixing orifice
6. Aerosol sampling head
7. Test device pressure tap
8. Test device
9. Test device pressure tap
10. Mixing orifice (efficiency testing)
11. Aerosol sampling head
12. HEPA filtration (optional)
13. Example of upper air flow nozzle pressure tap (optional)
14. Example of air flow measurement device location
15. Example of lower air flow nozzle pressure tap

Figure 4. *Schematic diagram of the test rig (ISO 16890:2016, Part 2, 2016, p. 17)*

To get a better understanding of possible influence of electrostatic forces to the filtration efficiency, the filtration efficiency test is done two times. First time the test is done with unconditioned element, which may contain electrostatic charges. Before the second test, the element is conditioned to be antistatic. Conditioning is done by using isopropanol (IPA), which is vaporized in a separate conditioning cabinet. After conditioning, the filtration efficiency test is run again with the conditioned element. The average efficiency, which is used for classifying the filter, is calculated as a mean of these two efficiency tests. (ISO 16890:2016, Part 4, 2016, pp. 5-8)

To be able to measure the dust loading capacity of the filter, the test rig must have a dust injection nozzle installed, which delivers the dust from the dust feeder. (ISO 16890:2016, Part 3, 2016, pp. 11-12) The used test dust is L2 which is specified in ISO 15957. Dust is fed to the tested filter at a concentration of 140 mg/m^3 and the pressure difference over the filter is measured during the feeding. Initial arrestance of the filter is determined by

the first 30 g of dust and the additional dust increments give information about the arrestance versus dust loading until the final resistance. Final resistance is set to 200 Pa for coarse filters and to 300 Pa for finer filters. (ISO 16890:2016, Part 3, 2016, pp. 16-17)

3.2.2 Classification system

Compared to EN 779 -standard, the classification system of ISO 16890 is completely different. ISO 16890 classifies filters to four groups: Coarse, ePM_{10}, $ePM_{2,5}$ and ePM_1. To which group the filter belongs is depending on the filtration efficiency with specific sized particles. Filters are classified to group "coarse" if their filtration efficiency is <50 % with 10 µm particles. If filter's filtration efficiency is ≥50 % with 10 µm particles it belongs to group ePM_{10}. Filters with filtration efficiency of ≥50 % with 2,5 µm particles belongs to group $ePM_{2,5}$, and likewise if efficiency is ≥50 % with 1 µm particles it belongs to group ePM_1. (ISO 16890:2016, Part 1, 2016, p. 15)

After the group name, there is also shown the percentage of filtration efficiency at that specific particle size, e.g. ISO $ePM_{2,5}$ 70 %, meaning in this case that the filter has 70 % efficiency with 2,5 µm particles. The percentage is rounded downwards to the closest multiply of 5 %. Because of the new structure of ISO 16890 classification system, the same filter can be classified to several different groups. The same filter can be for example ISO ePM_1 65 % and also ISO ePM_{10} 95 %. This multi-classification feature helps in choosing the right filter to the right application. (ISO 16890:2016, Part 1, 2016, p. 15)

The different classes of ISO 16890 are illustrated in Table 3:

Table 3. *ISO 16890 classification system (Jalkanen, et al., 2017, p. 129)*

ISO ePM$_1$	**ISO ePM$_{2,5}$**	**ISO ePM$_{10}$**	**ISO Coarse**
50 %	50 %	50 %	Initial gravimetric arrestance
55 %	55 %	55 %	
60 %	60 %	60 %	
65 %	65 %	65 %	
70 %	70 %	70 %	
75 %	75 %	75 %	
80 %	80 %	80 %	
85 %	85 %	85 %	
90 %	90 %	90 %	
95 %	95 %	95 %	
>95 %	>95 %	>95 %	

3.3 EN 1822:2009 – High efficiency air filters (EPA, HEPA and ULPA)

EN 1822:2009 standard is valid for EPA (Efficient Particulate Air Filter), HEPA (High efficiency Particulate Air Filter) and ULPA (Ultra Low Penetration Air Filter) filters, and it consists of five different parts:

- Part 1 – Classification, performance testing, and marking
- Part 2 – Aerosol production, measuring equipment, and particle counting statistics
- Part 3 – Testing flat sheet filter media
- Part 4 – Determining leakage of filter elements (scan method)
- Part 5 – Determining the efficiency of filter elements

This standard is used to determine the filtration efficiency of the filter, but it does not provide information about the dirt holding capacity of the filter.

3.3.1 Testing process and test rig

Testing in standard EN1822:2009 is based on particle counting methods. The efficiency is defined by counting particles at the most penetrating particle size (MPPS). MPPS is the particle size that has the lowest filtration efficiency and it is in the range of 0,15 µm to 0,3 µm. Because of the small particle size, it is possible to test also ultra-low penetration air filters (ULPA). (Wilcox, et al., 2010, p. 86)

Tests are done by using liquid test aerosol. Recommended aerosols to use are DEHS, PAO or PSL, but also other aerosols are allowed. Solid aerosol is allowed to use for leak testing. In each of the tests, the test aerosol can be either monodisperse aerosol where all the particles are same sized, or polydisperse aerosol where there is a size distribution among particles. The concentration and the size distribution of the aerosol should be constant, and for the leak and efficiency tests the size of the particles should be the most penetrating particle size (MPPS) as average. (EN 1822:2009. Part 1, p. 9)

For counting the particles, there are two different methods which can be used. Total count method (CNC) counts the total number of particles but does not take account the particle sizes. Other option is to use particle size analysis method (OPC) which counts the number of particles separately for each particle size. The type of counting method and the test aerosol type must be chosen so that they are aligned and are functional together. (EN 1822:2009. Part 1, pp. 9-10)

EN1822:20019 includes three different testing methods for filters. Each of these tests can be run independently as they test different things. First test consists of testing the filter media as a sheet. Test is done to determine the most penetrating particle size (MPPS) which is needed in the other two tests. The test must be made with six different particle sizes. If monodisperse aerosol is used, test must be run six times with different particle size each time to be able to determine the MPPS. Minimum of five test samples are needed, and the MPPS is determined as the mean size, based on the samples. (EN 1822:2009. Part 1, pp. 9-13)

In the second test, filters are tested for absence of leaks at their nominal air volume flow rate. Second test is done for filters in groups H and U. Group H filter elements can be tested by any of the three leak test methods mentioned in the EN 1822-4. Group U filter elements must be tested for leaks using the MPPS scanning method mentioned in the EN 1822-4. (EN 1822:2009. Part 1, p. 9) In scanning method particle penetration is measured with a sampling tube which is circled around the element so that the sampling tube takes measurements from the whole filter surface area. If there are manufacturing irregularities or leakages in the element, the particle flow rate will rise and therefore indicate about the leakage. (EN 1822:2009. Part 4, p. 7)

In the third test, the integral efficiency of the tested filter element is determined using MPPS test aerosol. There are two methods mentioned in the standard to test the integral efficiency. In both methods the sample from the upstream is taken by a fixed sampling probe. In the first method there is also a fixed probe installed to the downstream of the filter element. The efficiency of the filter is calculated from the particle count of these probes, from the sampling duration and from the sampling volume flow rate. The second method is the same scanning method that is used in the leakage test described before. Therefore, the test results from the leakage test can be used to calculate also the filter's integral efficiency. (EN 1822:2009. Part 5, 2009, pp. 7-8)

The test rig according to standard 1822:2009 is illustrated in Figure 5:

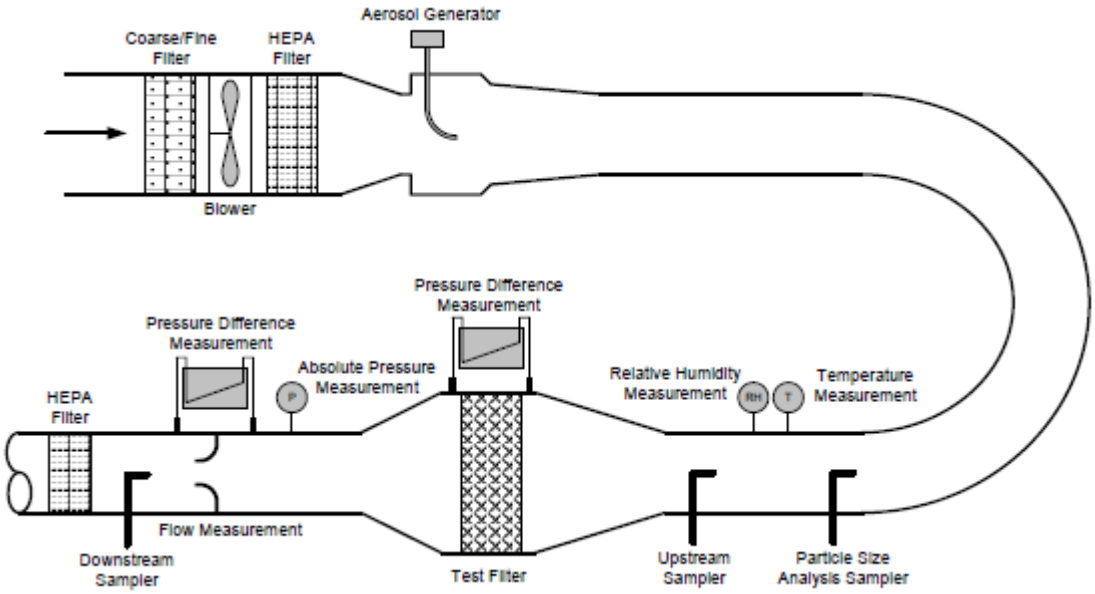

Figure 5. *Schematic of EN 1822:2009 Efficiency test set-up (Wilcox, et al., 2010, p. 87)*

3.3.2 Classification system

Filters are classified in groups E, H and U in standard EN 1822. These groups are subdivided into classes E10-E12, H13-H14 and U15-U17. Group E filters are EPA filters (Efficient Particulate Air Filter), group H filters are HEPA filters (High efficiency Particulate Air Filter), and group U filters are ULPA filters (Ultra Low Penetration Air Filter). (EN 1822:2009. Part 1, p. 6) Filter classes and their requirements are shown in Table 4:

Table 4. *Classification of EPA, HEPA and ULPA filters (EN 1822:2009. Part 1, p. 10)*

Filter Class	Integral value		Local value	
	Efficiency [%] of MPPS	**Penetration [%] of MPPS**	**Efficiency [%] of MPPS**	**Penetration [%] of MPPS**
E10	≥ 85	≤ 15	Group E filters cannot and shall not be leak tested for classification purposes.	
E11	≥ 95	≤ 5		
E12	≥ 99,5	≤ 0,5		
H13	≥ 99,95	≤ 0,05	≥ 99,75	≤ 0,25
H14	≥ 99,995	≤ 0,005	≥ 99,975	≤ 0,025
U15	≥ 99,9995	≤ 0,0005	≥ 99,9975	≤ 0,0025
U16	≥ 99,99995	≤ 0,00005	≥ 99,99975	≤ 0,00025
U17	≥ 99,999995	≤ 0,000005	≥ 99,9999	≤ 0,0001

As is shown in the table, filters are classified only by their filtration efficiency.

3.4 Eurovent 4/9:1997 - Method of testing air filters used in general ventilation for determination of fractional efficiency

Eurovent 4/9 -standard is used to determine fractional efficiency of the filter, and it supersedes the older Eurovent 4/5 -standard. (Eurovent 4/9:1997, p. 1) Eurovent 4/9 -standard provides more complete knowledge of filter characteristics, especially about the fractional analysis. The standard is valid for air filters used in general ventilation, with face velocity of >0,6 m/s. (Eurovent 4/9:1997, p. 5)

3.4.1 Testing process and test rig

There are several square section ducts in the test rig, see Figure 6. The test rig must be executed so that stable aerosol with homogenous concentration is obtained. (Eurovent 4/9:1997, p. 8)

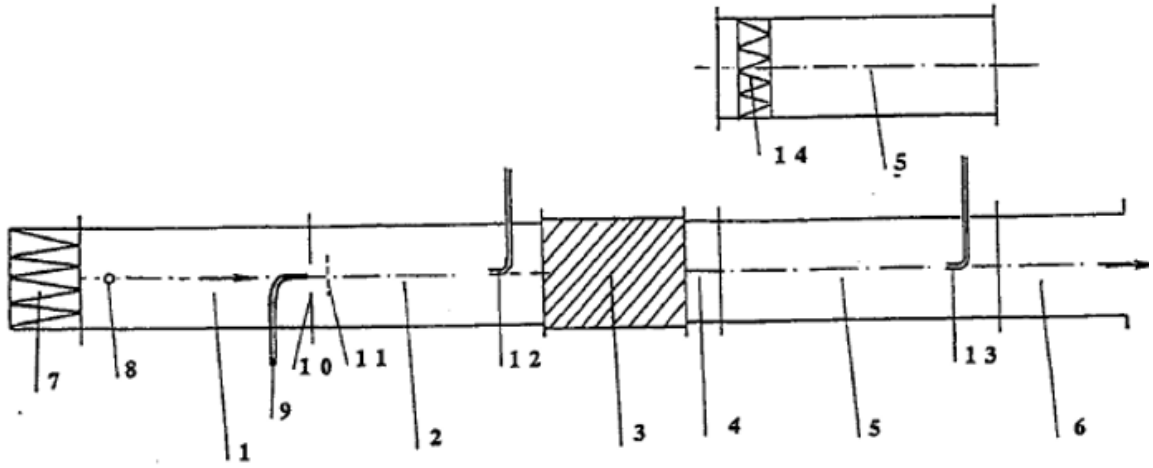

1. Duct part of the test rig
2. Duct part of the test rig
3. Duct part of the test rig
4. Duct part of the test rig
5. Duct part of the test rig
6. Duct part of the test rig
7. HEPA filter
8. Inlet point for DEHS or LATEX particles
9. Dust feeding probe
10. Mixing orifice
11. Perforated plate
12. Upstream sampling head
13. Downstream sampling head
14. Final filter for dust weight arrestance test

Figure 6. *Eurovent 4/9 test rig (Eurovent 4/9:1997, p. 23)*

In the first duct there is a HEPA filter to filter the inlet air of the test rig. After the HEPA filter, the aerosol is dispersed. (Eurovent 4/9:1997, p. 8) There is a dust feeding probe located in the second duct and it produces synthetic dust to the testing system at constant rate. With linear dust feeder, a specified amount of dust is loaded into a mobile dust feed tray. The tray moves at constant speed and delivers the dust to a paddle wheel which carries the dust to a slot of a dust pick-up tube of an ejector. The dust is dispersed in the ejector with compressed air, and is then directed to the testing system via dust feeder tube. (Eurovent 4/9:1997, p. 12)

A perforated plate after the dust feeder ensures that the particle distribution is uniform. After the plate and just before the tested filter is an upstream sampling head, which calculates the particles before the filtration. (Eurovent 4/9:1997, p. 8)

The tested filter is installed in the third duct. In duct 5 there is a downstream sampling head to measure the dirt particles after the filtration. For arrestance test, there is also a final filter which should be mounted so that the removal of the filter causes no disturbance to the filter or to the test rig. (Eurovent 4/9:1997, p. 8)

Tests can be run in under-pressure or in over-pressure depending on the placement of the fan. (Eurovent 4/9:1997, p. 8) Filter collection efficiency is calculated by measuring particles from both sides of the filter with laser particle counting method. The measured particle sizes vary from ≤0,2 µm to 3 µm. (Eurovent 4/9:1997, p. 4)

The pressure drop over the tested filter is measured with at least four different flow rates: 50 %, 75 %, 100 % and 125 % of rated air flow. The filtration efficiency test contains a series of 13 measurements of one minute each. To keep the particle concentration as homogeny as possible there is a one-minute purge or a one-minute period without measuring the particles before each one-minute measurement period. The particle collection for calculations is executed with tapered probes installed in the center of the upstream and downstream sides of the tested filter. (Eurovent 4/9:1997, p. 13)

To determine the dust holding capacity and weight arrestance of the filter, the tested filter is loaded with synthetic test dust. The used test dust is ASHRAE-type standardized dust which is generated to the system at a concentration of 70 mg/m^3. After the dust loading test, the final filter from the end side of the test rig is removed and weighted to be able to determine the amount of dirt particles that have not been filtered by the tested filter. By comparing the weight of the final filter before and after the dust loading test, the weight arrestance of the tested filter can be calculated. (Eurovent 4/9:1997, p. 14)

3.4.2 The test rig in Parker Hannifin's laboratory in Urjala

The test rig in the laboratory of Parker Hannifin's Urjala location is based on the Eurovent 4/9 standard. However, even though the test rig is based on the standard, there are some differences between the standard and the test rig built in the laboratory. The major difference is the lack of dust feeder in the Urjala's test rig. Therefore, it is not able to measure the dust holding capacity or the weight arrestance of the tested filter.

The test rig used in Parker Hannifin's laboratory in Urjala is illustrated in Figure 7:

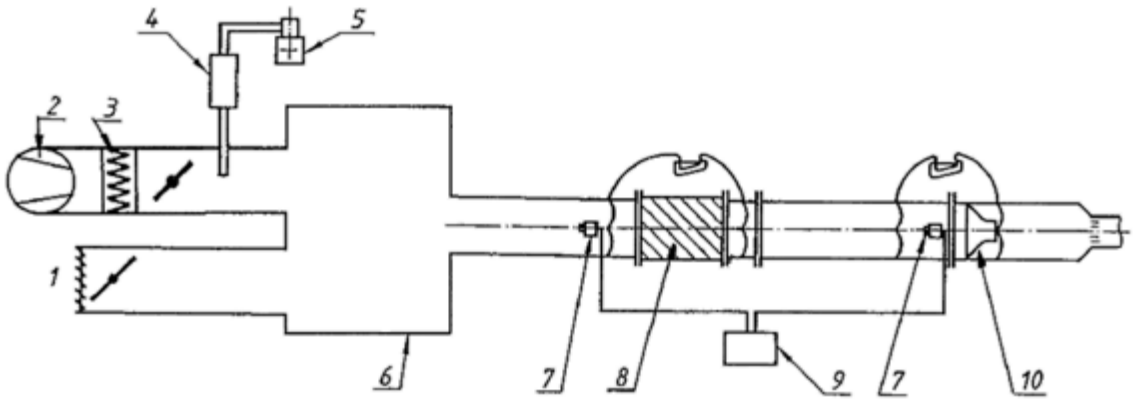

1. Air in
2. Fan
3. HEPA filter
4. Aerosol neutralizer (not in use)
5. Aerosol generator
6. Mixing chamber
7. Sampling
8. Test filter
9. Particle analyzer
10. Volume flow meter

Figure 7. *Test rig used in Parker Urjala laboratory*

3.4.3 Classification system

Eurovent 4/9 classification system is aligned with the classification system of EN 779-standard. Both standards have the same requirements for different filter classes, even though the filter classes have different names in each standard. Eurovent 4/9 classifies the filters to classes EU1-EU9 depending on their filtration efficiency with 0,4 µm particles. If the filtration efficiency is less than 40 % with 0,4 µm particles, the class of the filter depends on the arrestance level of the test dust. (Eurovent 4/9:1997, p. 42) The different filter classes and their requirements are shown in Table 5.

Table 5. *Classification according to Eurovent 4/9 (Eurovent 4/9:1997, p. 42)*

Group	Eurovent 4/9 class	Average arrestance [%], synthetic dust	Average efficiency [%], 0,4 µm particles
Coarse	EU1	$A_m < 65$	
Coarse	EU2	$65 \leq A_m < 80$	
Coarse	EU3	$80 \leq A_m < 90$	
Coarse	EU4	$90 \leq A_m$	
Fine	EU5		$40 \leq E_m < 60$
Fine	EU6		$60 \leq E_m < 80$
Fine	EU7		$80 \leq E_m < 90$
Fine	EU8		$90 \leq E_m < 95$
Fine	EU9		$95 \leq E_m$

The tests which these classifications are based on are done under the same conditions as with EN779-standard: air flow Q = 0,944 m^3/s (3400 m^3/h), maximum final test pressure drop for coarse filters (classes EU1-EU4) Δp = 250 Pa, and maximum final test pressure drop for fine filters (classes EU5-EU9) Δp = 450 Pa.

3.5 Comparison of the standards

In Table 6 all the key parameters of the standards presented in chapters 3.1 - 3.4 are collected into a single table:

Table 6. *Comparison table of the standards*

	EN 779:2012	**ISO 16890:2016**	**EN 1822:2009**	**Eurovent 4/9:1997**
Particle size	0,4 µm (0,2 – 3 µm)	0,3 – 10 µm	MPPS (0,15 – 0,3µm)	0,4 µm (0,2 – 3 µm)
Dust holding capacity	Yes	Yes	No	Yes (not in Urjala's test rig)
Pressure loss	Yes	Yes	Yes	Yes
Classes	Coarse: (G1 – G4) Medium: (M5 – M6) Fine: (F7 – F9)	ISO Coarse ISO ePM_{10} ISO $ePM_{2,5}$ ISO ePM_{1}	EPA: (E10 – E12) HEPA: (H13 – H14) ULPA: (U15 – U17)	Coarse: (EU1 – EU4) Fine: (EU5 – EU9)
Test aerosol	DEHS	DEHS (<1 µm) KCI (2,5 µm – 10 µm)	DEHS, PAO, PSL or alterna-tive	DEHS
Test dust	ASHRAE	L2 (ISO 15957)	-	ASHRAE

4. FILTRATION MECHANISMS OF GAS FILTRATION

Filtration can be thought as a two-step process. First of all, the dirt particle must be captured from the passing flow. The second step is to avoid the captured particle to escape from the collector. The ability to keep the collected particle captured, also known as particle adhesion, depends on the interaction between the particle and the collector surface. The interaction is affected for example by collector surface geometry and material characteristics. (Tien, 2012, p. 198)

Particle collection efficiency consists of two factors: the efficiency of capturing the particle and the probability to hold the particle captured. (Tien, 2012, p. 198) Mathematically this can be expressed as:

$$\eta = \eta_C * \gamma,$$

where η_C is the capturing efficiency and γ is the probability of particle adhesion. In most cases the probability of particle adhesion is very high, and therefore it is often ignored in the calculations. (Tien, 2012, p. 199) This is also the case in the simulation model presented in chapter 5; the probability of losing the captured particle is not included in the calculations as a separate parameter.

There are several different mechanisms to capture the particle from the passing flow. Particle can be captured by interception, inertial impaction, diffusion, combined effect of interception and diffusion, gravity or by electrostatic forces.

4.1 Interception

Particles are captured by interception because their size is finite. If there were no external forces acting on the particle, the particle would coincide with the fluid streamlines. (Tien, 2012, p. 205) If the distance between the particle's streamline (i.e. the center of the particle) and collector's surface is less than the radius of the particle, the particle will be captured by the collector due to interception. (Wang & Tronville, 2014, p. 3) The mechanism of interception is illustrated in Figure 8.

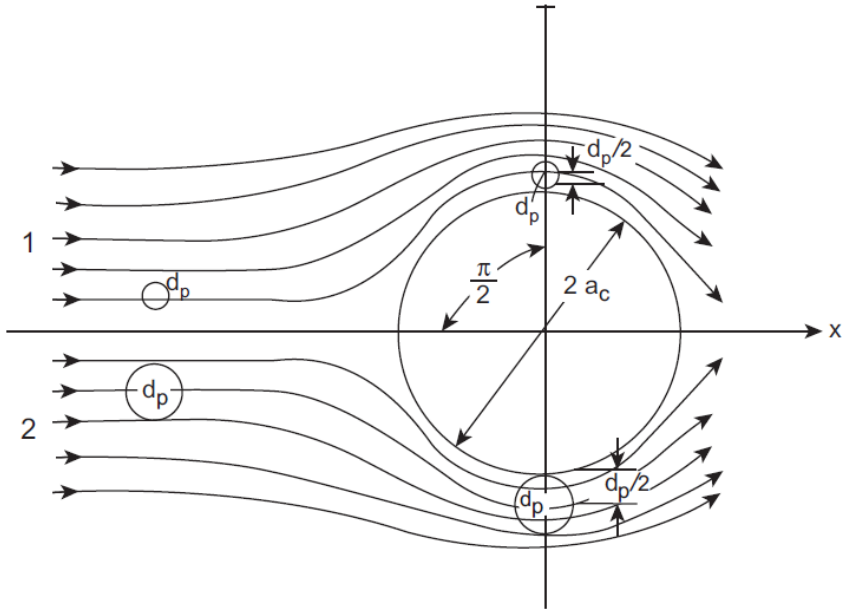

Figure 8. *Particle deposition caused by interception (Tien, 2012, p. 205)*

In the streamline 1 of the Figure 8 the particle is not captured by the collector, because particle's center is more than the radius of the particle away from the surface of the collector. In other words, the surface of the particle does not touch the surface of the collector. In streamline 2 the particle's streamline is less than the particle's radius away from the collector's surface. Therefore, the particle is captured by the collector. (Wang & Tronville, 2014, p. 6).

The efficiency of the interception is depending on the particle sizes. The larger the particles are, the more likely they are being captured by interception. (Wang & Tronville, 2014, p. 6). Interception is the only filtration mechanism where the particle is not diverging from the original gas streamline (Hinds, 1999, p. 192).

4.2 Inertial impaction

Inertial impaction is one of the most important mechanism of particle deposition for micron-sized aerosol particles. In Figure 9 is shown the inertial effect, where the gas flow is illustrated over a cylindrical collector (e.g. fiber). (Tien, 2012, p. 199)

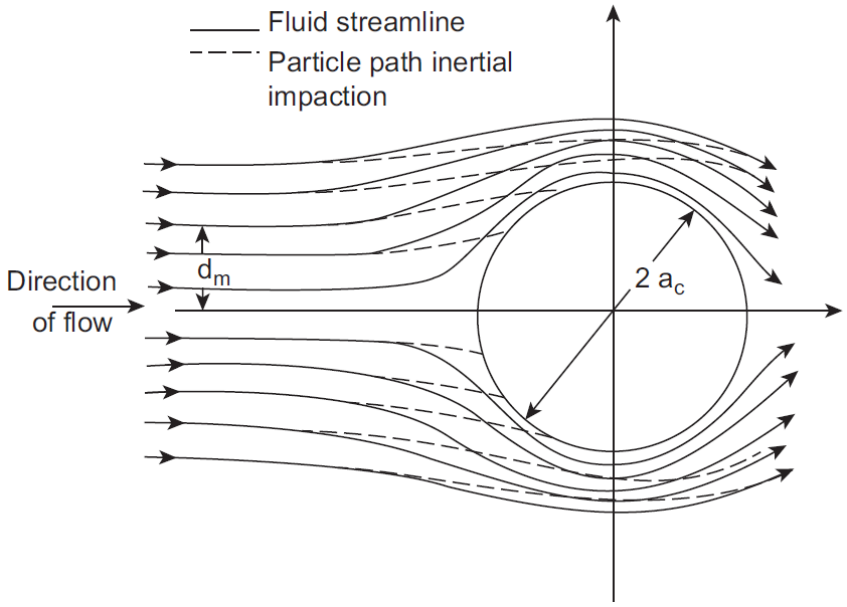

Figure 9. *Particle deposition caused by inertial impaction (Tien, 2012, p. 199)*

The movement of the flow, containing fluid and particles, is rectilinear when in remote distance from the collector. In the proximity of the collector, the fluid streamlines begin to arch away from the collector in order to avoid collision with the collector. However, the particles of the flow behave differently compared to the fluid. Because of particles' inertia, they do not change their streamlines so efficiently. As a result, some of the particles streamlines collide with the collector's surface, and therefore particles are captured by the collector. (Tien, 2012, pp. 199-200)

The larger the particle size is, the bigger the effect of inertial impaction is (Wang & Tronville, 2014, p. 6). The effect of inertial impaction is also greater in high velocity applications (Wilcox, et al., 2010, p. 10).

4.3 Diffusion

To be able to understand the diffusion mechanism of filtration, first is needed to understand the Brownian motion. Brownian motion is random motion of the particles caused by molecules of the fluid. The particles collide with molecules around the particle, and these collisions causes the particles to move randomly in every direction. (Law & Rennie, 2015)

The diffusion filtration mechanism involves the dirt particles being captured because of the random movement of the particles caused by Brownian motion (Wang & Tronville, 2014, p. 3). In the Figure 10 is illustrated the effect of Brownian motion to the dirt particles.

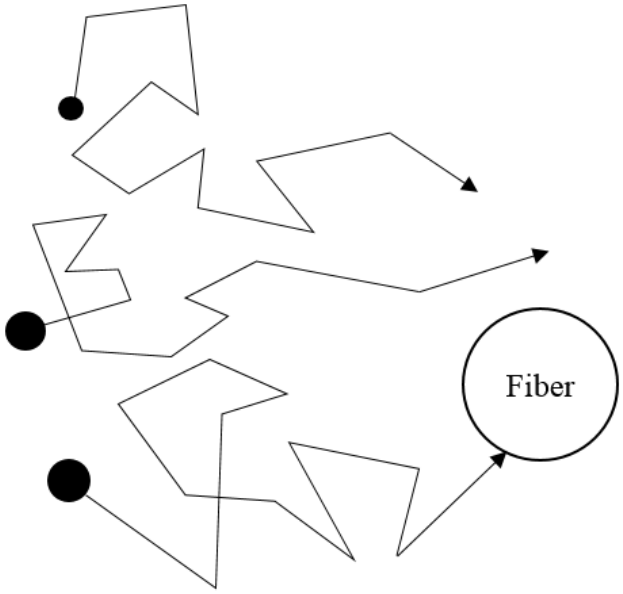

Figure 10. *Dirt particles under the influence of Brownian motion*

Because of random movement caused by Brownian motion, some of the dirt particles collides with the collector and are therefore captured by the collector. This filtration mechanism is called diffusion or Brownian diffusion.

For nanoparticles without electrostatic forces, the diffusion is the main mechanism of particle filtration (Tien, 2012, p. 207). The effect of particle filtration by diffusion increases as the size of the particles decreases and therefore it works best with particles well below 100 nm. (Wang & Tronville, 2014, pp. 6, 19-20). It is the only filtration mechanism where the filtration efficiency increases as the particle size decreases (Hinds, 1999, p. 195). Low flow rate of the fluid increases the effect of diffusion furthermore (Wilcox, et al., 2010, p. 10).

4.4 Combination of interception and diffusion

In addition to interception and diffusion acting individually, these two mechanism are considered to have also a combined effect to the filtration efficiency. It is considered to be an interaction term to account for the enhanced collection due to interception of the diffusing particles (Hinds, 1999, p. 195).

4.5 Gravity

Because the particle density is greater than the fluid density, also gravity has influence to the particle movement. The particle may settle out in the direction of gravitational force. (Tien, 2012, p. 204) Gravitational settling may change the streamlines of the particle

movement and the particle can therefore be captured by the collector. However, the influence of the gravity is relevant only for larger particles above a few micrometers and at low velocity. (Wang & Tronville, 2014, p. 4)

4.6 Electrostatic forces

In addition to mechanical capture mechanisms, particles may also be captured by electrostatic forces. If the filter or the aerosol that is being filtered possess electrostatic charges, it will have effect to filtration efficiency. (Wang & Tronville, 2014, p. 4)

There are several different mechanisms of electrostatic forces influencing the filtration efficiency:

1. The Coulombic force between charged particles and charged collectors, F_{EC}
2. The electric image force between charged particles and neutral collectors, F_{EI}
3. The electric image force between neutral particles and charged collectors, F_{EM}
4. The force on charged particles in the presence of a neutral collector by a uniform external electric field, F_{EX}
5. The particle charged in the same sign produces a repulsive force among themselves, F_{ES}
6. The electric dipole interaction force between an uncharged particle and an uncharged collector both being polarized by an external electric field, F_{icp}
   (Tien, 2012, p. 213)

The total electrostatic force F_E is defined as the sum of all the individual forces:

$F_E = F_{EC} + F_{EI} + F_{EM} + F_{EX} + F_{ES} + F_{icp}$. (Tien, 2012, p. 213)

Filters that collect particles in both mechanical and electrostatic mechanisms, are called electret filters (Sun, 2008, p. 1) Filtration efficiency of electret filters increases with lower face velocity and smaller fiber diameter. Decreasing filter thickness, fiber charge or the packing density of the filter media decreases the efficiency of electret filter. The single fiber efficiency can be calculated by combining the mechanical efficiency of the filter with the efficiency due to electrical forces. (Huang, et al., 2013, p. 163) The formula of the combined efficiency is defined as:

$$E_{\Sigma m,e} = 1 - \left(1 - E_{\Sigma m,sf}\right) * (1 - E_{\Sigma e,sf}),$$

where $E_{\Sigma m,sf}$ = total single fiber efficiency due to mechanical force, and $E_{\Sigma e.sf}$ = total single fiber efficiency due to electrical force. (Huang, et al., 2013, p. 163)

Because of these additional mechanisms to capture particles, electret filters tend to have better efficiency than conventional filters (Huang, et al., 2013, p. 164). The greater the

electric charge of the filter media is, the better the filter efficiency by electrostatic attraction will be. However, the correct charge configuration is important. With wrong configuration, the filtration efficiency will decrease. The charge level of the filter may also vary with time and use. (Wang & Tronville, 2014, p. 4)

5. MATHEMATICAL MODEL FOR FILTER PERFORMANCE SIMULATION

Each of the filtration mechanisms presented in chapter 4 can be simulated with mathematical formulas. The mathematical simulation model of this study combines these different filtration mechanisms and formulas into a single model. The simulation model will give information about the filter's capability by simulating the filtration efficiency and the pressure loss of the filter media.

There are several different input parameters in the model which can be altered: properties of the filter media, type of gas, temperature, pressure, flow velocity and particle density. By varying these parameters, filter's capability can be simulated in many different scenarios.

The simulation model is also useful for comparing filters which are performing with different gases. The model includes three different gases: air, nitrogen and methane. Methane is considered to be equivalent to natural gas in the simulation, because of natural gas's high concentration of methane (see chapter 2.1). The simulation model takes account three gas parameters in the calculations: molar mass, dynamic viscosity and density. These gas properties are presented in Table 7:

Table 7. *Table of gas properties*

	Air	**Nitrogen**	**Methane**
Molar mass [kg/mol]	0,0289644	0,0280134	0,0160425
Dynamic viscosity [kg/ms] @ 21 °C, 1 bar	1,82E-05	1,76E-05	1,11E-05
Density [kg/m^3] @ 21 °C, 1 bar	1,20088	1,1457	0,65715

The original version of the simulation model was received from IUTA, and it was further developed in this study. The simulation model is implemented as a separate excel-file, and the user interface of the model is illustrated in appendix A.

5.1 Filtration efficiency formulas

Filtration efficiency of the filter is calculated by combining the efficiencies of each different filtration mechanism.

5.1.1 Total filtration efficiency

The filtration efficiency of the filter (E) is the fraction of the dirt particles captured by the filter media. It expresses how efficient the filter is with specific dirt particle size. The efficiency is defined as:

$$E = (1 - P) * 100, \quad (1)$$

where P = fraction of the unfiltered dirt particles. (Wang & Tronville, 2014, p. 2) The fraction of the dirt particles not captured by the filter media is calculated as:

$$P = e^{-\frac{4*\alpha*E_{\Sigma,sf}*t}{\pi*(1-\alpha)*d_f}} \quad (2)$$

where α = packing density of the filter; $E_{\Sigma,sf}$ = total single fiber efficiency; t = thickness of the filter [m], and d_f = fiber diameter [m]. (Wang & Tronville, 2014, p. 3)

Because of the complexity of fibrous filtration, the filtration must be simulated by calculating the filtration efficiency of a single fiber. The single fiber efficiency ($E_{\Sigma,sf}$) is the ratio of the number of particles captured by a single fiber to the number of particles in the volume of air geometrically swept out by the fiber. (Hinds, 1999, p. 190) The total single fiber efficiency is the sum of all the different dirt particle capturing mechanisms including interception, inertial impaction, diffusion, enhanced collection due to interception of the diffusing particles, and gravity (Wang & Tronville, 2014, p. 3). It is defined as:

$$E_{\Sigma,sf} = E_{R,sf} + E_{I,sf} + E_{D,sf} + E_{DR,sf} + E_{G,sf}, \quad (3)$$

where E_R = single fiber efficiency due to interception; E_I = single fiber efficiency due to inertial impaction; E_D = single fiber efficiency due to diffusion; E_{DR} = single fiber efficiency due to interception and diffusion combined, and E_G = single fiber efficiency due to gravitation. (Wang & Tronville, 2014, p. 3) The total single fiber efficiency is limited by the ratio of particle diameter and fiber diameter:

$$E_{\Sigma,sf} = \begin{matrix} 1 + N_R, if\ E_{\Sigma,sf} > 1 + N_R \\ E_{\Sigma,sf}, if\ E_{\Sigma,sf} \leq 1 + N_R \end{matrix}, \quad (4)$$

where N_R = ratio of particle and fiber diameters, and is therefore defined as:

$$N_R = \frac{d_p}{d_f}, \quad (5)$$

where d_p = particle diameter [m], and d_f = fiber diameter [m]. (Hinds, 1999, p. 192)

5.1.2 Filtration efficiency due to diffusion

Filtration efficiency due to diffusion can be calculated as:

$$E_D = (1 - P_D) * 100, \quad (6)$$

where E_D = efficiency due to diffusion, and P_D = portion of the particles not filtered due to diffusion. Portion of the unfiltered particles is calculated as:

$$P_D = e^{-\frac{4*\alpha*E_{D,sf}*t}{\pi*d_f}}, \quad (7)$$

where α = packing density of the filter; $E_{D,sf}$ = single-fiber efficiency due to diffusion; t = thickness of the filter [m], and d_f = fiber diameter [m]. (Wang & Tronville, 2014, p. 3)

The formula of the single fiber efficiency due to diffusion ($E_{D,sf}$) varies between different studies (Wang & Tronville, 2014, p. 3). The formula used in the simulation model is defined as:

$$E_{D,sf} = 2{,}6 * (\frac{1-\alpha}{K_u})^{\frac{1}{3}} * Pe^{-\frac{2}{3}} \quad (8)$$

where α = packing density of the filter; K_u = Kuwabara hydrodynamic factor, and Pe = Peclet number [ ]. (Lee & Liu, 1982, p. 151) Peclet number (Pe) expresses the relative importance of convection and diffusion (Wang & Tronville, 2014, p. 3). It is defined as:

$$Pe = \frac{U_0*d_f}{D}, \quad (9)$$

where U_0 = filtration face velocity [m/s], d_f = fiber diameter [m], and D = diffusion coefficient. (Hinds, 1999, p. 194) Diffusion coefficient is defined as:

$$D = \frac{k*T*C_c}{3*\pi*\mu*d_p}, \quad (10)$$

where k = Boltzmann constant [J/K]; T = temperature [K]; C_c = slip correction factor; μ = dynamic viscosity [kg/ms], and d_p = particle diameter [m]. (Wang & Tronville, 2014, p. 3)

When using continuum model for fluid simulation with high-efficiency filter media, the slip effect must be taken account for more accurate simulation results. Otherwise the continuum approximation of the gas flow around the fiber is not working accurately. Slip

correction factor (C_c) is used to improve the accuracy of continuum model approximation. (Dhaniyala & Liu, 1999, p. 42), and it is defined as:

$$C_c = 1 + \frac{Kn_p}{2} * (2{,}34 + 1{,}05 * e^{-0{,}39*\frac{2}{Kn_p}}), \quad (11)$$

where Kn_p = Knudsen number. (Hinds, 1999, p. 49)

Knudsen number is the ratio of mean free path and the fiber diameter. It is a dimensionless parameter which indicates whether the continuum mechanism can be used to model fluid simulation or if some other mechanism must be used. Fluid can be treated as a continuous medium if the Knudsen number is below 0,1. (Talbot, 2014) As the Knudsen number rises over 0,1, the simulation results start to suffer. When the Knudsen number is over 0,2, the continuum model should be replaced by molecular model. (Bird, 1995, p. 2)

Knudsen number is defined as:

$$Kn_p = \frac{2*\lambda}{d_f}, \quad (12)$$

where λ = mean free path, and d_f = fiber diameter [m]. (Dhaniyala & Liu, 1999, p. 42)

Mean free path (λ) expresses the average travelled distance of a particle between collisions with the molecules of the gas (Law & Rennie, 2015). This is illustrated in Figure 11:

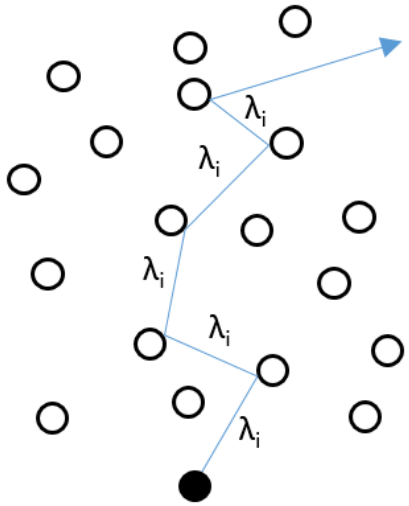

Figure 11. *Mean free path*

As the pressure of the gas rises, also the density of the gas increases. This leads to more frequent collisions and therefore to smaller mean free path. Mean free path is calculated as:

$$\lambda = \sqrt{\frac{\pi * R * T}{8 * M}} * \frac{\mu}{0{,}5 * p}, \quad (13)$$

where R = gas constant $[\frac{j}{mol*K}]$; T = temperature [K]; M = molar mass [kg/mol]; μ = dynamic viscosity [kg/ms], and p = pressure [Pa]. (Tien, 2012, p. 180)

5.1.3 Filtration efficiency due to inertial impaction

Filtration efficiency due to inertial impaction (E_I) is calculated as:

$$E_I = (1 - P_I) * 100, \quad (14)$$

where P_I = portion of the particles not filtered due to inertial impaction. Portion of the unfiltered particles due to inertial impaction is determined as:

$$P_I = e^{-\frac{4 * \alpha * E_{I,sf} * t}{\pi * d_f}}, \quad (15)$$

where α = packing density of the filter; $E_{I,sf}$ = single fiber efficiency due to inertial impaction; t = thickness of the filter [m], and d_f = fiber diameter [m]. (Wang & Tronville, 2014, p. 3)

The single fiber efficiency due to inertial impaction ($E_{I,sf}$) is defined as:

$$E_{I,sf} = \frac{Stk * J}{2 * {K_u}^2}, \quad (16)$$

where Stk = Stokes number; J = experimental parameter, and K_u = Kuwabara hydrodynamic factor. (Hinds, 1999, p. 194) $E_{I,sf}$ is limited to be

$$E_{I,sf} = \begin{matrix} 1 + N_R, if\ E_{I,sf} > (1 + N_R) \\ E_{I,sf}, if\ E_{I,sf} \leq (1 + N_R) \end{matrix}, \quad (17)$$

where N_R = ratio of particle and fiber diameter. (Hinds, 1999, p. 194)

Parameter J is defined as:

$$J = \begin{matrix} (29{,}6 - 28\alpha^{0{,}62}) * {N_R}^2 - 27{,}5{N_R}^{2{,}8}, if\ N_R \leq 0{,}4 \\ 2, if\ N_R > 0{,}4 \end{matrix}, \quad (18)$$

where α = packing density of the filter, and N_R = ratio of particle and fiber diameters. (Hinds, 1999, p. 194)

Stokes number (Stk) indicates the significance of the inertial impaction (Tien, 2012, p. 201). If Stokes number is high, the particle will not follow the flow stream, and will instead continue its movement straight to the fiber and get captured, because of the inertia of the particle (Wang & Tronville, 2014, p. 3). Stokes number (Stk) is defined as:

$$Stk = \frac{\rho_p * {d_p}^2 * C_c * U_0}{18 * \mu * d_f}, \quad (19)$$

where ρ_p = particle density [kg/m^3]; ρ_g = gas density [kg/m^3]; dp = particle diameter [m]; Cc = slip correction factor; U_0 = filtration face velocity [m/s]; μ = dynamic viscosity [kg/ms], and d_f = fiber diameter [m]. (Hinds, 1999, p. 193)

5.1.4 Filtration efficiency due to interception

The filtration efficiency due to interception (E_R) can be calculated as:

$$E_R = (1 - P_R) * 100, \quad (20)$$

where P_R = portion of the particles not filtered due to interception. Portion of the unfiltered particles due to interception is defined as:

$$P_R = e^{-\frac{4 * \alpha * E_{R,sf} * t}{\pi * d_f}}, \quad (21)$$

where α = packing density of the filter; $E_{R,sf}$ = single fiber efficiency due to interception; t = thickness of the filter [m], and d_f = fiber diameter [m]. (Wang & Tronville, 2014, p. 3)

The formula for the single fiber efficiency due to interception ($E_{R,sf}$) is defined as:

$$E_{R,sf} = \frac{1-\alpha}{K_u} * \frac{{N_R}^2}{1+N_R}, \quad (22)$$

where α = packing density of the filter; N_R = ratio of particle and fiber diameter, and K_u = Kuwabara hydrodynamic factor. (Lee & Liu, 1982, p. 152)

Kuwabara hydrodynamic factor (K_u) expresses the effect of neighboring fibers to the flow around the fiber (Wang & Tronville, 2014, p. 3). It is defined as:

$$K_u = -0{,}5 * \ln(\alpha) - 0{,}75 - 0{,}25\alpha^2 + \alpha, \quad (23)$$

where α = packing density of the filter. (Lee & Liu, 1982, p. 151)

5.1.5 Filtration efficiency due to interception of diffusing particles

Interception of diffusing particles is an additional filtration mechanism to improve the simulation accuracy with particle sizes near MPPS. (Hinds, 1999, p. 195) The filtration efficiency due to it is defined as:

$$E_{DR} = (1 - P_{DR}) * 100, \quad (24)$$

where E_{DR} = efficiency due to interception and diffusion combined, and P_{DR} = portion of the particles not filtered due to interception and diffusion combined. Portion of the unfiltered particles due to interception of diffusing particles (P_{DR}) is calculated as:

$$P_{DR} = e^{-\frac{4*\alpha*E_{DR,sf}*t}{\pi*d_f}}, \quad (25)$$

where α = packing density of the filter; $E_{DR,sf}$ = single fiber efficiency due to interception of diffusing particles; t = thickness of the filter [m], and d_f = fiber diameter [m]. (Wang & Tronville, 2014, p. 3)

The single fiber efficiency due to interception of diffusing particles ($E_{DR,sf}$) is calculated as:

$$E_{DR,sf} = \frac{1{,}24*N_R^{\frac{2}{3}}}{\sqrt{Pe*K_u}}, \quad (26)$$

where N_R = ratio of particle and fiber diameters; Pe = Peclet number [ ], and K_u = Kuwabara hydrodynamic factor. (Hinds, 1999, p. 195)

5.1.6 Filtration efficiency due to gravity

The formula for the filtration efficiency due to gravitation (E_G) is:

$$E_G = (1 - P_G) * 100, \quad (27)$$

where P_G = portion of the particles not filtered due to gravitation. Portion of the unfiltered particles is calculated as:

$$P_G = e^{-\frac{4*\alpha*E_{G,sf}*t}{\pi*d_f}}, \quad (28)$$

where α = packing density of the filter; $E_{G,sf}$ = filtration efficiency due to gravitation; t = thickness of the filter [m], and d_f = fiber diameter [m]. (Wang & Tronville, 2014, p. 3)

The single fiber efficiency due to gravity ($E_{G,sf}$) can be calculated with a formula defined as:

$$E_{G,sf} = G * (1 + N_R), \quad (29)$$

where G = gravitation parameter, and N_R = ratio of particle and fiber diameters. (Kirsh, 2001, p. 68) Parameter G is defined as:

$$G = \frac{\rho_p * {d_p}^2 * C_c * g}{18 * \mu * U0}, \quad (30)$$

where ρ_p = particle density [kg/m^3]; d_p = particle diameter [m]; C_c = slip correction factor; g = gravitational constant [m/s^2]; μ = dynamic viscosity [kg/ms], and U_0 = filtration face velocity [m/s]. (Hinds, 1999, p. 195)

5.2 Pressure drop formulas

The pressure drop of the filter media (Δp) can be calculated as:

$$\Delta p = F_d * \frac{4\alpha}{\pi * {d_f}^2} * t, \quad (31)$$

where F_d = drag force; α = packing density of the filter; d_f = fiber diameter [m], and t = thickness of the filter [m]. (Wang & Tronville, 2014, p. 7) The drag force F_d is calculated as:

$$F_d = \frac{4 * \pi * \mu * U_0}{K_u}, \quad (32)$$

where μ = dynamic viscosity [kg/ms]; U_0 = filtration face velocity [m/s], and K_u = Kuwabara hydrodynamic factor. (Wang & Tronville, 2014, p. 8) By combining the formulas (31) and (32), the formula for the pressure loss of the filter can be written as:

$$\Delta p = \frac{16\alpha}{K_u * d_f^2} * \mu * U_0 * t, \quad (33)$$

where α = packing density of the filter; K_u = Kuwabara hydrodynamic factor; d_f = fiber diameter [m]; μ = dynamic viscosity [kg/ms]; U_0 = filtration face velocity [m/s], and t = thickness of the filter [m]. (Wang & Tronville, 2014, p. 8)

There are also other versions of formulas for pressure drop calculations. A more empirical formula to calculate pressure drop is:

$$\Delta p = \frac{\mu * U_0 * t * (64\alpha^{1,5} * (1 + 56\alpha^3))}{d_f^2}, \quad (34)$$

where μ = dynamic viscosity [kg/ms]; U_0 = filtration face velocity [m/s], and t = thickness of the filter [m]; α = packing density of the filter, and d_f = fiber diameter [m]. (Davies, 1973)

5.3 Quality factor

The performance level and the capability of the filter can be estimated with a quality factor Q_f. It compares the penetration (i.e. filtration efficiency) and the pressure loss of the filter media and results as a unitless number. It can be used to compare different filters with each other. The quality factor formula is defined as:

$$Q_f = \frac{-\ln(P)}{\Delta p}, \qquad (35)$$

where Q_f = quality factor; P = penetration, and Δp = pressure drop. Higher quality factor means better filtration media. The comparison of the filters must be made with the same particle size and flow velocity. (Hinds, 1999, p. 188)

6. VALIDATION OF THE SIMULATION MODEL

The simulation model is validated by comparing the simulation results with actual test results tested with Parker Hannifin's air test rig. The used test rig is based on Eurovent 4/9-standard and it is described in chapter 3.4. In the validation process, nine different filter medias were used. All the medias were tested with the Eurovent 4/9 -test rig, and also the parameters of these medias were inserted to the simulation model. The simulation results were then compared to the actual test results to get information about the accuracy of the simulation model.

The validation of the model was done with air, as there is no test rig available with natural gas as a fluid. The tests were made in atmospheric pressure. The temperature was 21 °C, and the free flow velocity before the filter was 0,2 m/s. All the tested medias were non-woven, glass fiber filtration medias.

6.1 Filtration efficiency

Filtration efficiency is simulated as the total efficiency of all the individual filtration mechanisms. The individual filtration efficiency of each of the mechanisms can also be presented in the model to find out more detailed information about the influences of each mechanism. However, the validation is done using only the total efficiency. The total simulated filtration efficiency and the efficiencies of all the individual filtration mechanisms are illustrated in Figure 12.

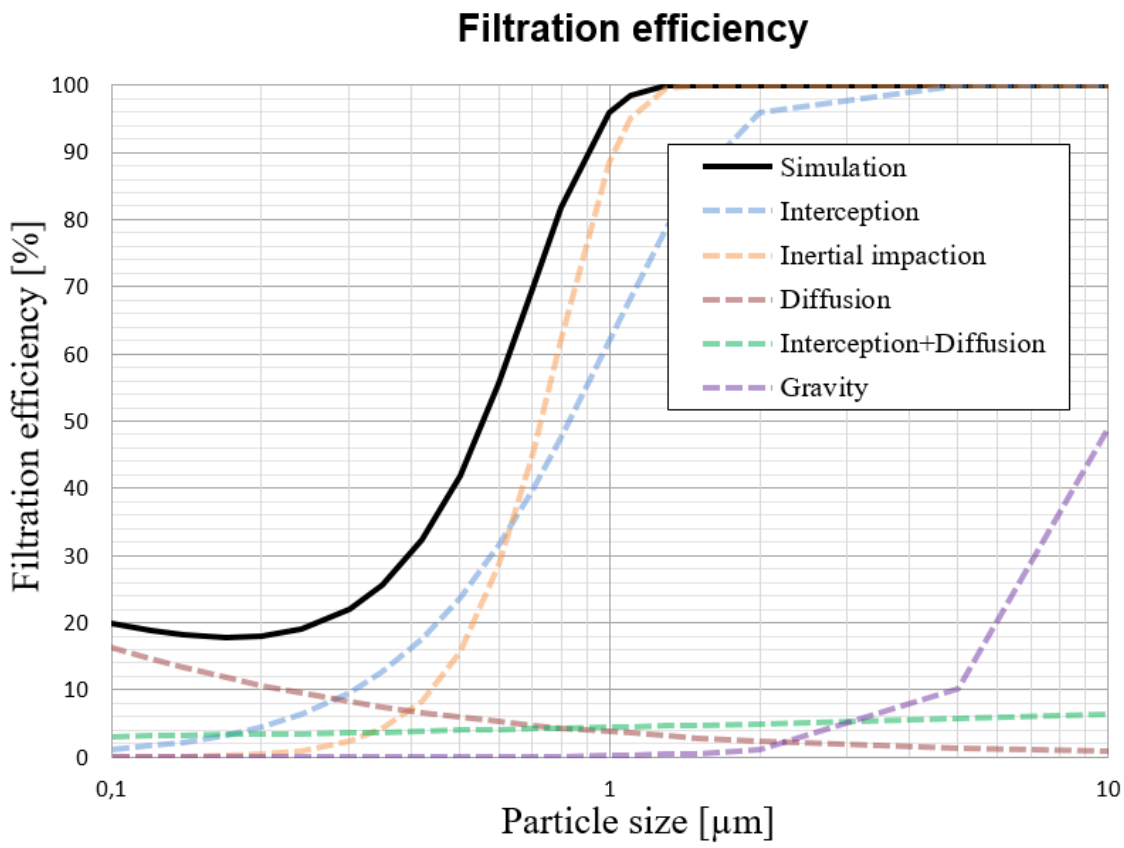

Figure 12. *Total and individual filtration efficiencies*

Test cycles were run 3 – 6 times per test, and filtration efficiency was counted as the average of the different cycles.

6.1.1 Tests with A4 samples

The filtration efficiency tests were made with unfolded A4-sized filter media samples. A total of nine different filter medias were tested, and below is presented the results of three of these medias. Filtration grade of the presented medias vary from coarse to fine.

The comparison of three different filtration medias and the test results from a test rig is presented in Figure 13 - Figure 15:

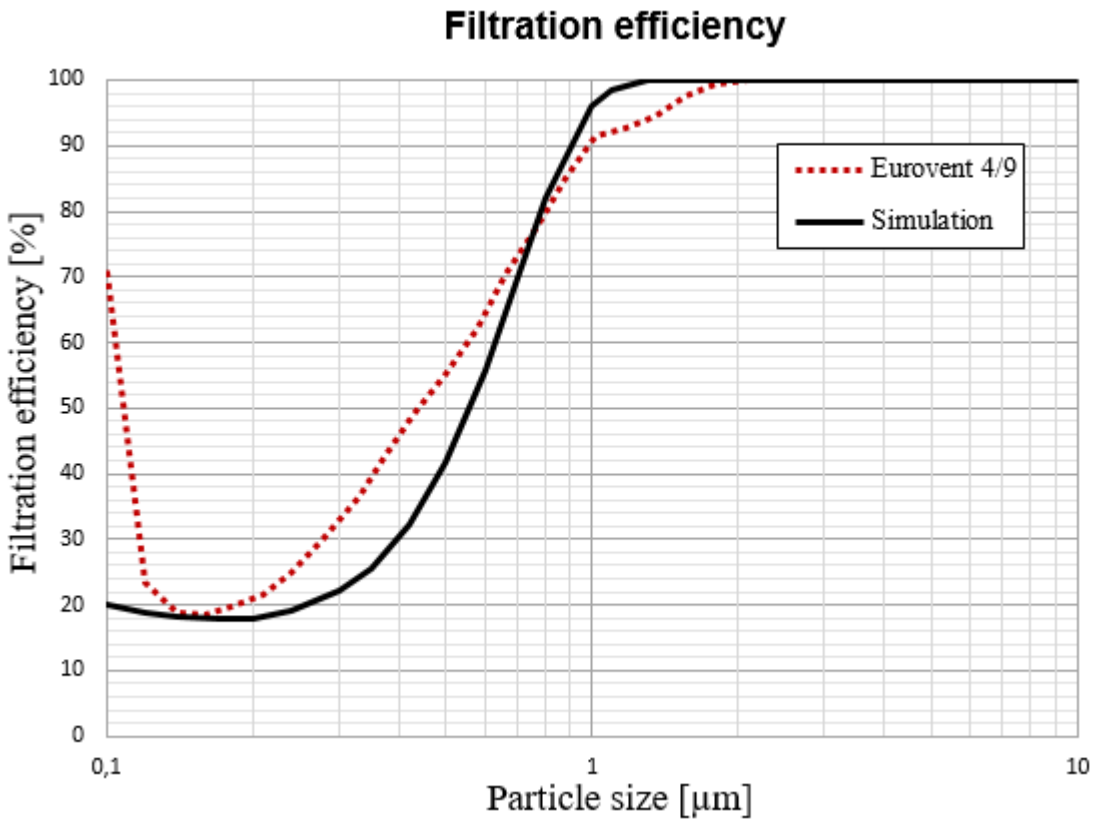

Figure 13. *Filtration efficiency, coarse media*

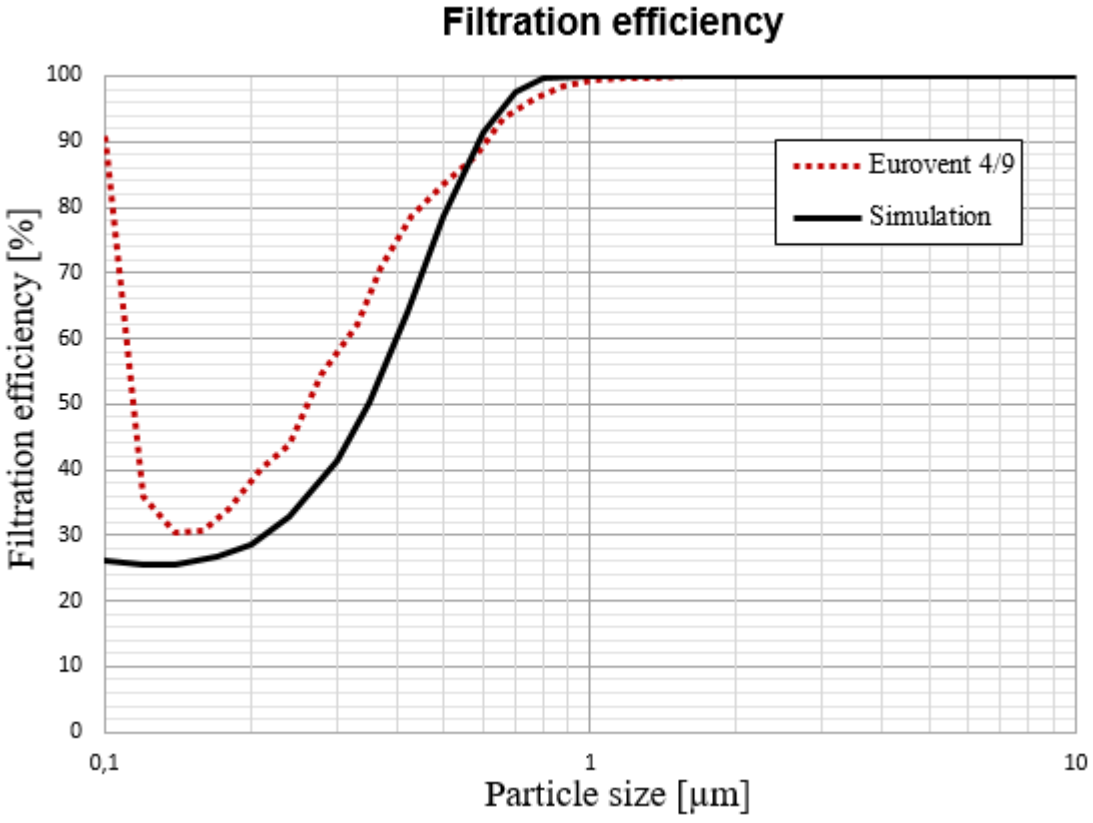

Figure 14. *Filtration efficiency, medium media*

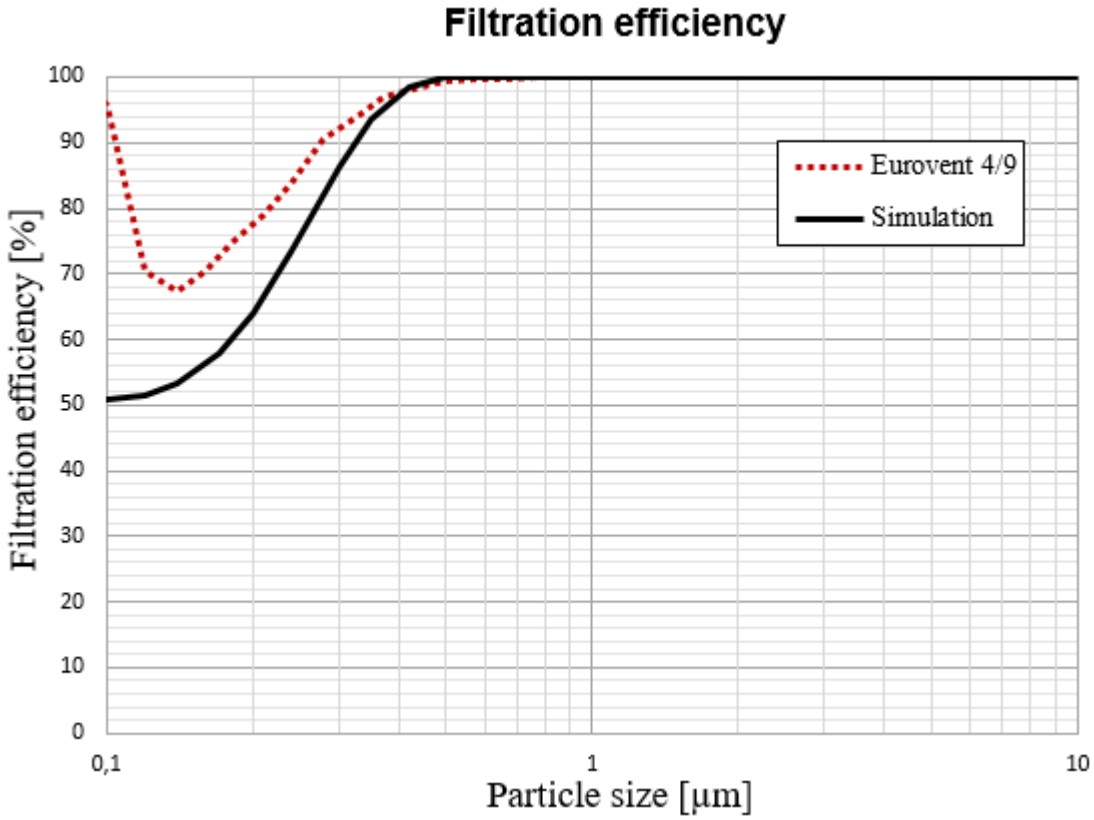

Figure 15. *Filtration efficiency, fine media*

In Figure 13 and Figure 14 the simulation results correspond with the Eurovent 4/9 -test rig results with good precision. There is a bigger gap between these two results only with the smallest particle sizes (0,10 – 0,12 µm), but otherwise the simulation accuracy is good.

With media 3 in Figure 15 there is a bigger difference between the results with particle sizes 0,1 – 0,2 µm, but the accuracy of the simulation is improved with particle sizes over 0,3 µm. The possible reasons for the differences are analyzed in chapter 6.3.

With every media, the shape of the simulated efficiency curve is truthful. In simulation and the test rig results, the filtration efficiency is high with very small particles (< 0,1 µm) and also with larger particles, but the efficiency decreases with medium sized particles. This results in a reverse bell shape curvature.

6.1.2 Tests with dual layer media

Filtration efficiency was simulated also with combined efficiency of two different filtration medias. This was done to validate the model in cases the filter has two different medias in a single filter element: fine media for filtration efficiency, and coarse media to improve the dirt holding capacity of the filter. Tests were made in the same conditions as with single layer of media, but with two medias on top of each other.

Test results compared to simulation results are illustrated in Figure 16 and Figure 17.

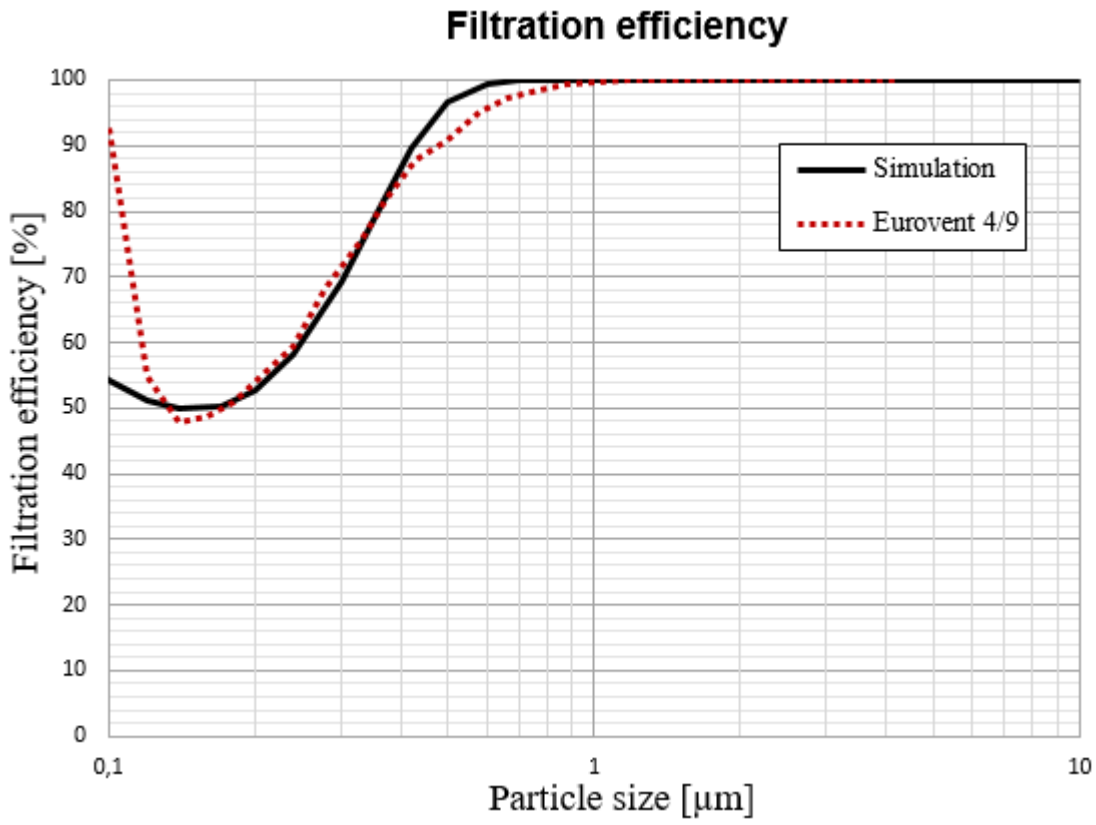

Figure 16. *Filtration efficiency, filter (medium) + pre-filter (coarse)*

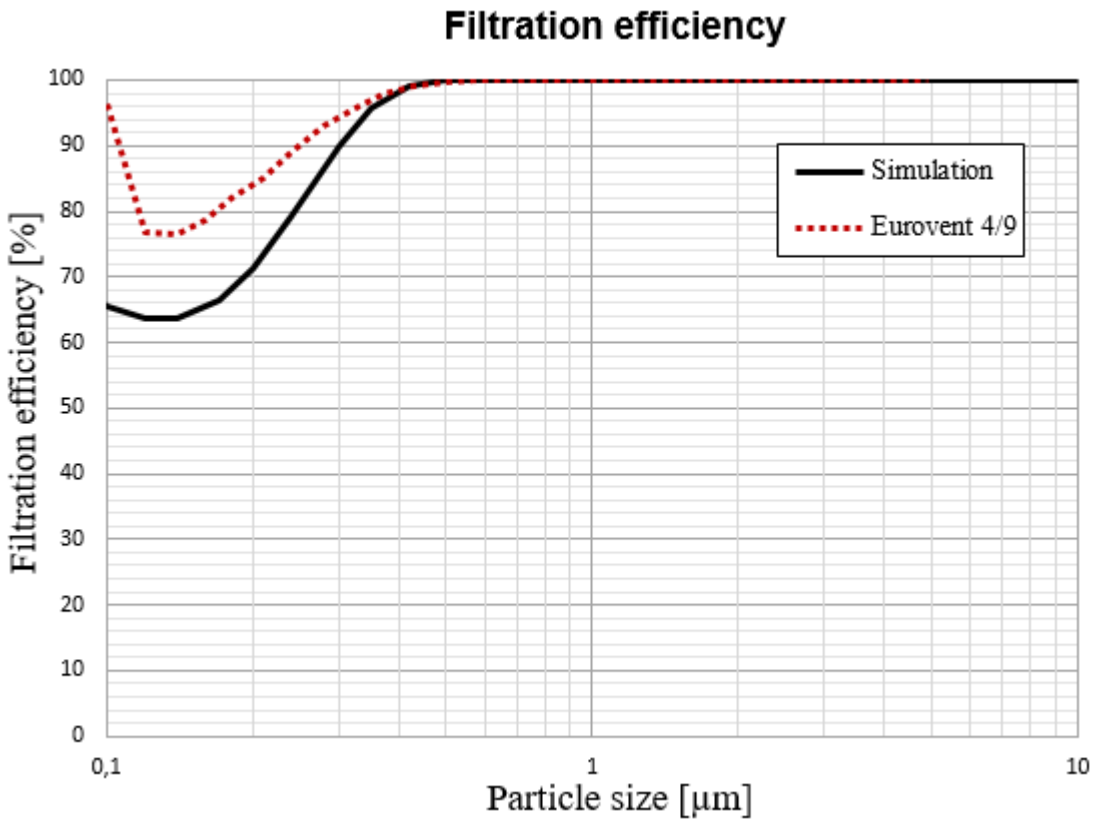

Figure 17. *Filtration efficiency, filter (fine) + pre-filter (coarse)*

In Figure 16 the simulation results correspond with the test rig results with high accuracy. The only significant difference between the two results are with the smallest particle sizes (0,10 – 0,12 µm), similarly to the single media validations in chapter 6.1.1.

The accuracy of the simulation model with two medias is only as accurate as it is with single medias. Possible inaccuracies with single media simulations reflect also to the dual media simulations. In Figure 17 there is similar kind of inaccuracies as can be seen with the individual simulation of the used two medias. The inaccuracies of the finer media are causing inaccuracies also to the dual layer simulation.

6.2 Pressure difference

In addition to filtration efficiency, also pressure loss can be simulated with the simulation model. In the testing rig, the pressure is measured before and after the filter. Pressure loss is the difference between these two measurements, and it is presented as a function of flow.

6.2.1 Tests with A4 samples

In Figure 18 and Figure 19 is presented the pressure losses of two different filtration medias:

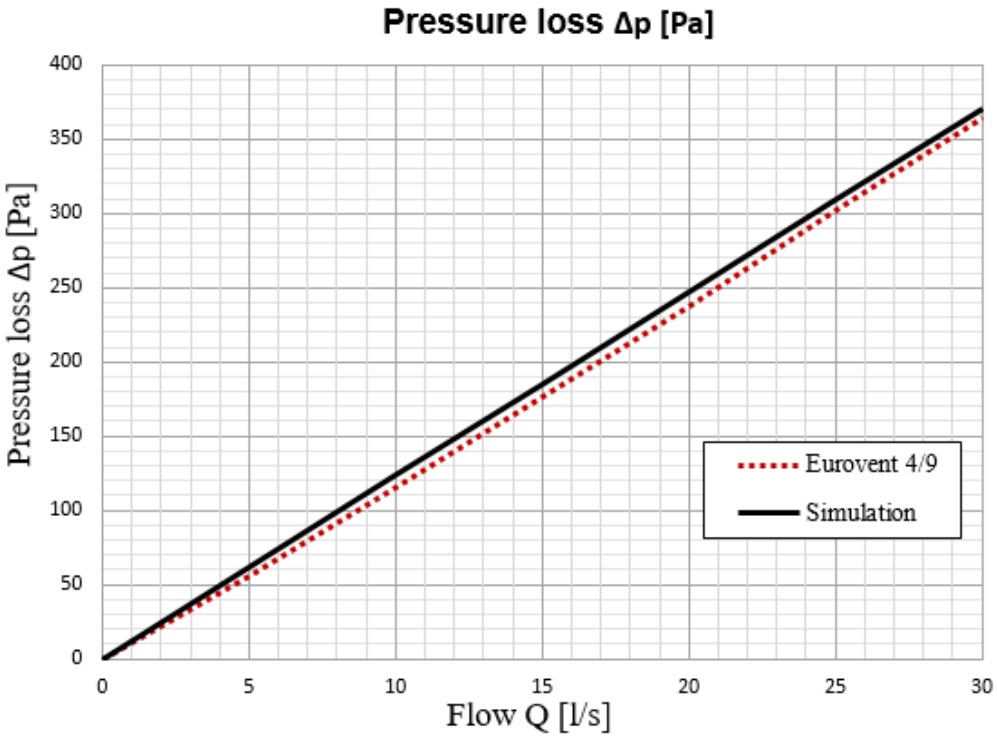

Figure 18. *Pressure loss, coarse media*

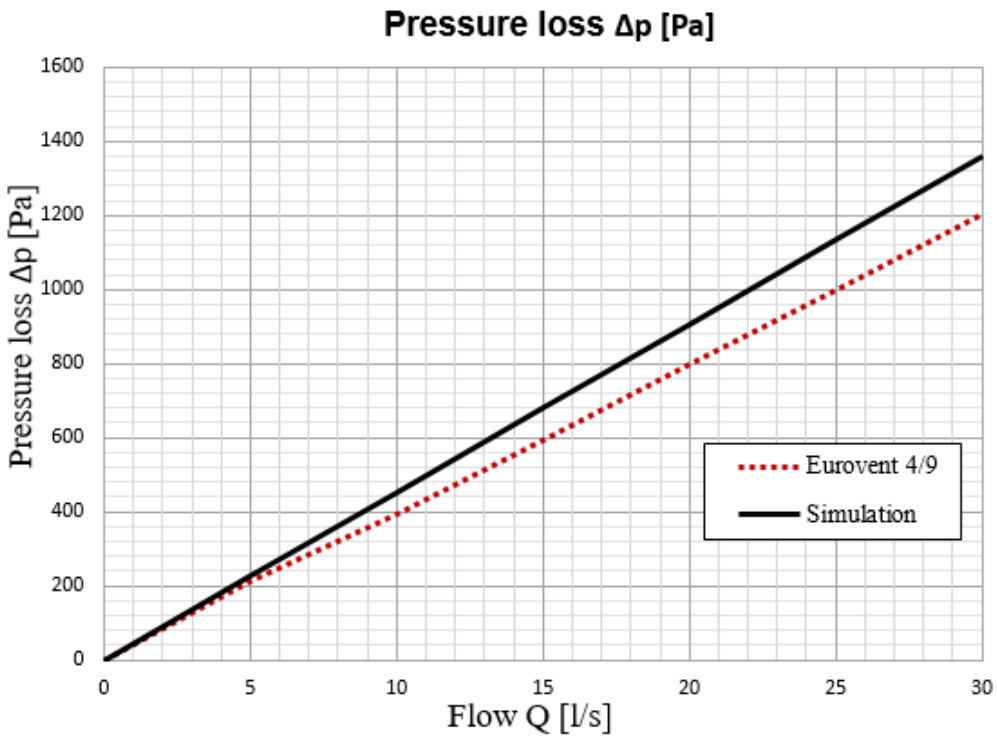

Figure 19. *Pressure loss, fine media*

The pressure loss rises as the flow increases, and the finer the media is, the bigger the pressure loss will be. The simulation model is very accurate with simulating the pressure loss. With most medias, the difference between the test rig result and the simulation result is very minor.

6.2.2 Tests with dual layer media

Dual layer medias were also tested for pressure loss, and the results are illustrated in Figure 20 and Figure 21.

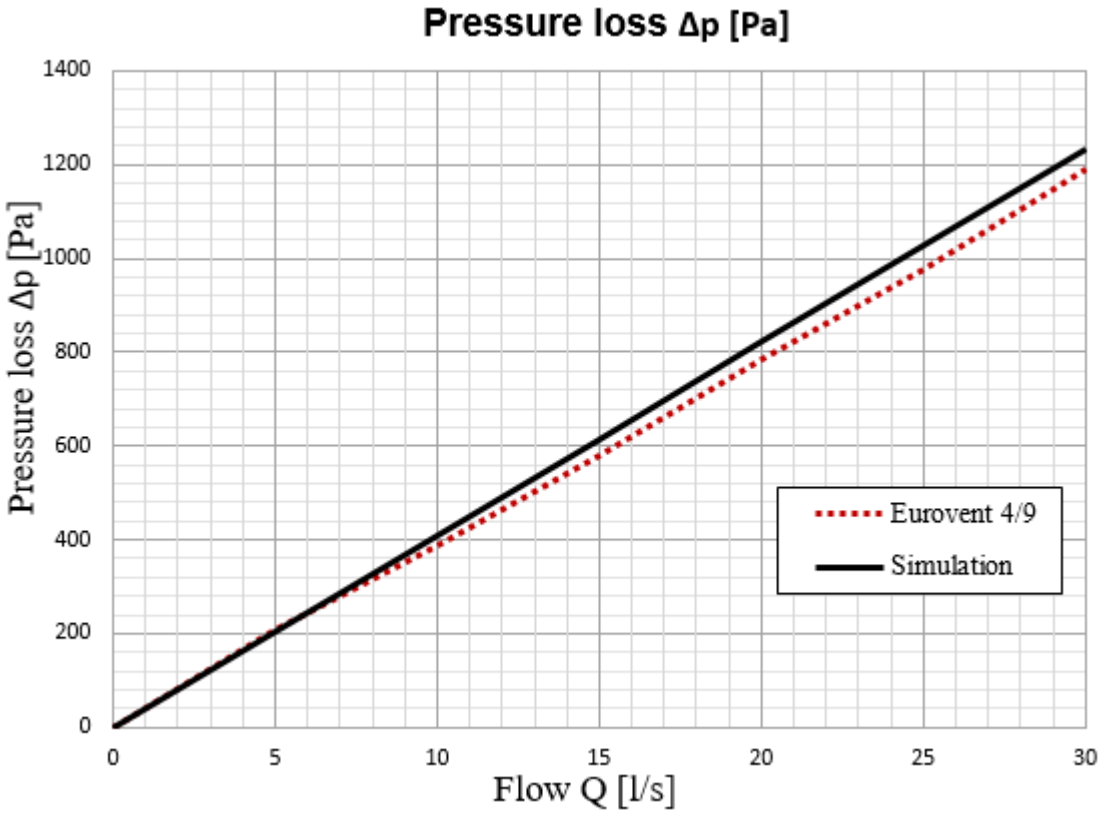

Figure 20. *Pressure loss, filter (fine) + pre-filter (coarse)*

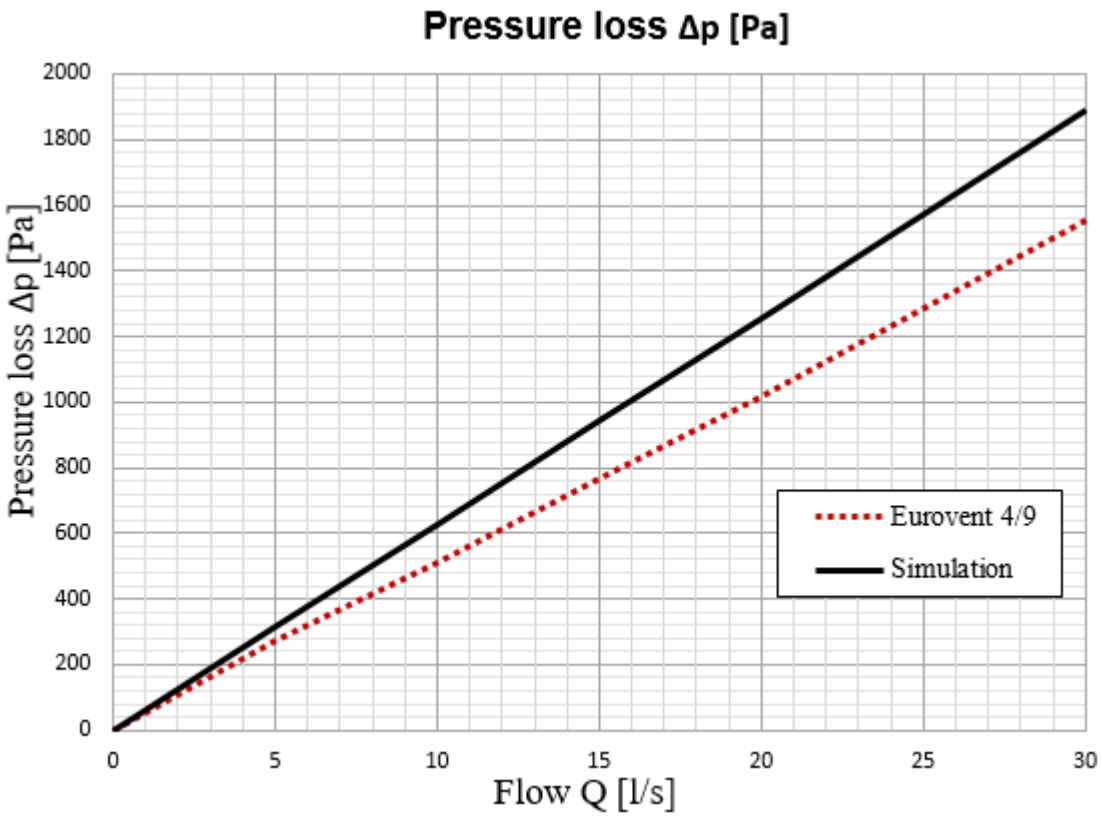

Figure 21. *Pressure loss, filter (fine) + pre-filter (coarse)*

For pressure loss simulations, the model works as accurate with dual layer medias as it works with single medias. If there are any inaccuracies with the individual filter media, it will affect also directly to accuracy of the dual media simulations.

6.3 Analyzing the differences

The general principles of air filtration are well known, but as air filtration is such a complicated process, there are still gaps between theory and experiments (Wang & Tronville, 2014, p. 2). The flow model and the different filtration mechanisms are only theoretical, and they do not reflect the reality with absolute accuracy. In different studies, there are several alternative formulas for the same filtration mechanisms. Some of the formulas are completely different, and some have different correction factors. There are also differences on how many filtration mechanisms are presented in the study, and in some studies there can be only two mechanisms included. These kind of big variances between the studies indicate that there is no single flawless theoretical model for gas filtration. The theoretical models are always simplifications of the complex reality.

The fibers in the non-woven filters are bonded together mechanically, thermally or chemically. Because the fibers are not manufactured for example by weaving or knitting, the orientation of the fibers are relatively random, although the main orientation of the fibers is perpendicular to the flow. In addition, the sizes of the fibers are uneven. (Wang &

Tronville, 2014, p. 2) Because of the random orientation and the inhomogeneity of the fibers, the actual flow deviates from the theoretical models (Lee & Liu, 1982, p. 148). The simulation model also considers the fibers to be cylindrical, and does not take into account the effect of lamination of the medias.

The validation of the simulation model is based on the test results from Parker Hannifin's test rig. However, there might be inaccuracies also in the test rig's results. To have better understanding of the accuracy of the test rig, same tests should be made also with some other test rig. Preferably, the tests should be made with a test rig which is based on a different standard. This would eliminate some of the procedural errors which possibly exist with the used standard.

Filtration efficiency is tested by running 3 – 6 test cycles, and filtration efficiency is the average of these cycles. By comparing filtration efficiencies of individual cycles, there can be seen major differences between the results. Differences are especially significant with the smallest particle sizes (0,09 – 0,12 µm). There are also significant differences with the smallest particle sizes between two different tests, which were performed similarly. This indicates that there is variance in the test results of the used test rig, and there might be significant inaccuracies especially with the smallest particle sizes.

Even though there are dissimilarities between the test rig results and the simulation results, the simulation model is working considerably accurate with most of the filtration medias. The accuracy of the model could be improved even further by modifying the formulas. Because of the complex and detailed structure of the simulation model, the model can be modified very diversely e.g. by adding correction factors to specific filtration mechanisms.

7. CONCLUSIONS

Unlike many other studies of gas filtration, in this study the gas filtration was not limited only to air filtration, but filtration was investigated also from natural gas aspect. Natural gas is a widely used source of energy, and its market share is growing. It is considered to be more environmental friendly than other fossil fuels. Before natural gas is available for the end user to use, it has gone complex processing procedures and has been transferred from far distances. During these processing procedures and transportation, the gas is purified from other gases, but also from solid dirt particles.

Natural gas is filtered at many stages, and the closer the gas is to the end user, the cleaner it usually is. Natural gas is used diversely in different kinds of applications. The use of natural gas ranges from industrial electricity generation to a cooking stove, and the cleanliness requirements of the gas are determined by the application.

Filters are often validated according to some standard. The standard describes a testing rig, which is used in the filter testing. If the filter is tested with a testing rig described in the standard, it can be classified to a specific class according to the standard. There are many different standards for air filter validation, but no standards specifically designed for filters working with some other gases than air. Because of the lack of specific standards, air filter standards must be used also for natural gas filters.

As there are no standards specifically designed for natural gas use, there are not any test rigs for natural gas testing available either. Therefore, filters must be tested with air. As the test results from air test rig only gives information about the filter's capabilities with air, the influence of the gas type to the filtration results must be estimated separately. In this study the estimation is done from a theoretical aspect with a simulation model.

The many studies of gas filtration have introduced numerous mathematical formulas to simulate gas flow and dirt particle separation. The formulas have been further developed in later studies, and when comparing the formulas to actual experiments, the accuracy has been improved. The studies introduce several different individual filtration mechanisms. By combining these different filtration mechanisms into a single simulation model, the filter's total filtration efficiency can be simulated.

With the simulation model, different kind of scenarios can be examined effortlessly by changing the input parameters of the model. The parameters include: type of gas, temperature, pressure, flow velocity, particle density, and the properties of the filtration media. With these inputs and the mathematical formulas, the model simulates the filtration efficiency and the pressure drop of the filter media.

The simulation model was validated by comparing the simulation results with the actual test results from Parker Hannifin's air test rig. There were a total of nine different filtration medias which were tested and simulated for this study. The comparison reveals that the model works relatively accurate with most of the tested filter medias. With the finest filter medias, the simulation results of filtration efficiency still need improving, but with coarser medias the efficiency simulations are very satisfactory. When simulating the pressure loss of a media, the simulation results were highly accurate with the majority of the filter medias.

The differences between the simulation model and the actual test results can be due to many different reasons. There are still some gaps between the theoretical formulas and the experiments. The simulation model does not reflect the absolute reality, and it simplifies many things. About the filter media, the model does not take into account the inhomogeneity of the fibers or the orientation of the individual fibers. Only the average diameter of the fiber is used, even though the actual sizes vary, and furthermore, the shape of the fiber is not actually perfectly cylindrical. The simulation model also ignores the layer of lamination on the filter media, which is manufactured to the media to hold the fibers together.

About the dirt particles, the simulation model takes account only the density of the particle and not e.g. the phase of the particle. In addition, the test rig should also be validated to get better understanding of the accuracy of it. This could be done by comparing the test results from the used test rig with some other test rig's results, to see how much variance there is.

Because of the complexity of the simulation model and the many formulas used in it, the model can be modified versatilely, e.g. by adding correction factors to the formulas, and manipulate the simulation results to correspond even better with the actual test results. By modifying the formulas, the simulation model is capable to give highly accurate results with all the filter medias, if needed.

REFERENCES

Azadi, M., Mohebbi, A., Scala, F. & Soltaninejad, S., 2011. Experimental study of filtration system performance of natural gas in urban transmission and distribution network: A case study on the city of Kerman, Iran. *Fuel 90,* pp. 1166-1171.

Bird, G., 1995. *Molecular gas dynamics and the direct simulation of gas flows.* New York: Oxford University Press.

Courtey, S., 2017. Definition of filtration performance - from EN 779 to ISO 16890. *REHVA Journal - February,* pp. 16-19.

Davies, C. N., 1973. *Air filtration.* London, New York: Academic Press.

Dhaniyala, S. & Liu, B. Y., 1999. Investigations of Particle Penetration in Fibrous Filters: Part II. Theoretical. *Journal of the IEST; Mar/Apr; 42, 2; Technology Collection,* pp. 40-46.

EN 1822:2009. Part 1, 2009. *High Efficiency Air Filters (EPA, HEPA and ULPA). Part 1: Classification, Performance Testing, Marking.* s.l.:European Committee for Standardization.

EN 1822:2009. Part 4, 2009. *High Efficiency Air Filters (EPA, HEPA and ULPA). Part 4: Determining Leakage of Filter Elemenents (Scan Method).* s.l.:European Committee for Standardization.

EN 1822:2009. Part 5, 2009. *High Efficiency Air Filters (EPA, HEPA and ULPA). Part 5: Determining the Efficiency of Filter Elements.* s.l.:European Committee for Standardization.

EN 779:2012, 2012. *Particulate air filters for general ventilation - Determination of the filtration performance.* s.l.:European Committee for Standardization.

Eurovent 4/9:1997, 1997. *Method of testing air filters used in general ventilation for determination of fractional efficiency.* s.l.:Eurovent/Cecomaf.

Guo, B. & Ghalambor, A., 2005. *Natural gas engineering handbook.* 1st toim. Houston: Gulf Publishing Company.

Hinds, W. C., 1999. *Aerosol technology : properties, behavior, and measurement of airborne particles.* 2nd toim. New York: Wiley.

Huang, S.-H.ym., 2013. Factors Affecting Filter Penetration and Quality Factor of Particulate Respirators. *Aerosol and Air Quality Research, 13,* pp. 162-171.

Hutten, I. M., 2007. *Handbook of Nonwoven Filter Media.* s.l.:Elsevier.

ISO 16890:2016, Part 1, 2016. *Air filters for general ventilation. Part 1: Technical specifications, requirements and classification system based upon particulate matter efficiency (ePM).* s.l.:European Committee for Standardization.

ISO 16890:2016, Part 2, 2016. *Air filters for general ventilation. Part 2: Measurement of fractional efficiency and air flow resistance.* s.l.:European Committee for Standardization.

ISO 16890:2016, Part 3, 2016. *Air filters for general ventilation. Part 3: Determination of the gravimetric efficiency and the air flow resistance versus the mass of test dust captured.* s.l.:European Committee for Standardization.

ISO 16890:2016, Part 4, 2016. *Air filters for general ventilation. Part 4: Conditioning method to determine the minimum fractional test efficiency.* s.l.:European Committee for Standardization.

Jalkanen, T. ym., 2017. *Ilmansuodattimien luokitus muuttuu.* s.l., s.n., pp. 127-132.

Kirsh, V., 2001. Gravitational Deposition of Aerosol Particles on a Fibrous Filter with Account for the Effect of Van der Waals Force. *Colloid Journal,* 63(1), pp. 68-73.

Law, J. & Rennie, R., 2015. *A Dictionary of Physics (7 ed.).* s.l.:Oxford University Press.

Lee, K. & Liu, B., 1982. Theoretical Study of Aerosol Filtration by Fibrous Filters. *Aerosol Science and Technology, 1:2,* pp. 147-161.

Mokhatab, S., Poe, W. A. & Mak, J. Y., 2015. *Handbook of Natural Gas Transmission and Processing.* s.l.:Elsevier.

Ouyang, M. & Liu, B., 1995. Analytical Solution of Flow Field and Pressure Drop for Filters with Noncircular Fibers. *Aerosol Science and Technology, 23:3,* pp. 311-320.

Speight, J. G., 2007. *Natural gas - A basic handbook.* 1st toim. Houston: Gulf Publishing Company.

Sun, C., 2008. *Mechanical or Electret Filters?.* Houston, s.n.

Suomen Kaasuyhdistys ry, 2014. *Maakaasukäsikirja.* Helsinki: s.n.

Talbot, L., 2014. *AccessScience: Knudsen number.* s.l.:McGraw-Hill Education.

Tien, C., 2012. *Principles of filtration.* s.l.:Elsevier.

Wang, J. & Tronville, P., 2014. *Towards standardized test methods to determine the effectiveness of filtration media against airborne nanoparticles.* Dordrecht: Springer Science+Business Media.

Wilcox, M., Baldwin, R., Garcia-Hernandez, A. & Brun, K., 2010. *Guideline for gas turbine inlet air filtration systems.* s.l.:Soutwest Research Institute.

Wood, D. A., Mokhatab, S. & Economides, M. J., 2008. *Technology option for securing markets for remote gas.* Grapevine, s.n.

Yu, C., 2013. *Physics 51A: Modern Physics,* California: University of California, School of Physical Sciences .

APPENDIX A: THE USER INTERFACE OF THE SIMULATION MODEL

Insert parameters:

Filter:	8	Choose from below table
Pre-filter:	1	Choose from below table
Type of gas:	1	Choose from below table
Temperature:	21	T [°C] (Limits: 0 - 26 °C)
Pressure:	1	p [bar] (Limits: 0 - 310 bar)
Free flow velocity before filter:	0,2	U0 [m/s]
Particle density:	912	ρp [kg/m³]

Number:	Supplier item no:	Item number:	Grade:	Generation:
1				
2				
3				
4				
5				
6				
7				
8				
9				
10				
11				

Type of gas:	1 = Air	2 = Nitrogen	3 = Methane

Gas parameters:		Molar mass		M [kg/mol]
		Dynamic viscosity		μ [kg/ms]
		Gas density		ρ [kg/m³]
Filter media parameters:		Packing density of the fi		α [ ]
		Fiber diameter		df [m]
		Thickness of the filter		t [m]
Physical constants:		Gravitation constant		g [m/s²]
		Gas constant		R [J/molK]
		Boltzmann constant		k [J/K]
Calculation factors:		Mean free path		λ [m]
		Knudsen number of fibe		Knp [ ]
		Kuwabara hydrodynamic		Ku [ ]
		RE Faser		[ ]
		Dp / Pa (Davis)		
Unit conversions:		Pressure		p [Pa = N/m²]
		Temperature		T [K]